Resveratrol and cyclodextrins, an easy alliance: Applications in nanomedicine, green chemistry and biotechnology

Philippe Jeandet,[a,b,*] Eduardo Sobarzo-Sánchez,[c,d] Md. Sahab Uddin,[e,b] Roque Bru,[f] Christophe Clément,[a] Cédric Jacquard[a], Seyed Fazel Nabavi[g], Maryam Khayat Kashani[g], Gaber El-Saber Batiha,[h] Haroon Khan,[i] Iwona Morkunas,[j] Mattheos Koffas[k], Franscesco Trotta[l], Adrian Matencio[l] and Seyed Mohammad Nabavi[g]

[a]*University of Reims Champagne-Ardenne, RIBP EA 4707 USC INRAE 1488, SFR Condorcet FR CNRS 3417, 51100 Reims Cedex, France*

[b]*Pharmakon Neuroscience Research Network, Dhaka, Bangladesh*

[c]*Laboratory of Pharmaceutical Chemistry, Faculty of Pharmacy, University of Santiago de Compostela, Campus Vida, 15782 Santiago de Compostela, Spain,*

[d]*Instituto de Investigación e Innovación en Salud, Facultad de Ciencias de la Salud, Universidad Central de Chile, Chile*

[e]*Department of Pharmacy, Southeast University, Dhaka, Bangladesh*

[f]*Plant Proteomics and Functional Genomics Group, Department of Agrochemistry and Biochemistry, Faculty of Science, University of Alicante, Alicante, Spain*

[g]*Applied Biotechnology Research Center, Baqiyatallah University of Medical Sciences, Tehran 14359-16471, Iran*

[h]*Department of Pharmacology and Therapeutics, Faculty of Veterinary Medicine, Damanhour University, Damanhour 22511, AlBeheira, Egypt*

[i]*Department of Pharmacy, Faculty of Chemical and Life Sciences, Abdul Wali Khan University Mardan, 23200, Pakistan.*

[j]*Department of Plant Physiology, Poznań University of Life Sciences, Wołyńska 35, 60-637 Poznań, Poland*

[k]*Dorothy and Fred Chau '71 Constellation Professor, Center for Biotechnology and Interdisciplinary Studies, Room 4005D, Rensselaer Polytechnic Institute, 110 8th Street, Troy, NY 12180, United States of America*

[l]*Department of Chemistry, University of Turin, via P. Giuria 7, 10125, Turin, Italy*

*Corresponding author: Philippe Jeandet, philippe.jeandet@univ-reims.fr

Most drugs or the natural substances reputed to display some biological activity are hydrophobic molecules that demonstrate low bioavailability regardless of their mode of absorption. Resveratrol and its derivatives belong to the chemical group of stilbenes; while stilbenes are known to possess very interesting properties, these are limited by their poor aqueous solubility as well as low bioavailability in animals and humans. Among the substances capable of forming nanomolecular inclusion complexes which can be used for drug delivery, cyclodextrins show spectacular physicochemical and biomedical implications in stilbene chemistry for their possible application in nanomedicine. By virtue of their properties, cyclodextrins have also demonstrated their possible use in green chemistry for the synthesis of stilbene glucosylated derivatives with potential applications in dermatology and cosmetics. Compared to chemical synthesis and genetically modified microorganisms, plant cell or tissue systems provide excellent models for obtaining stilbenes in few g/L quantities, making feasible the production of these compounds at a large scale. However, the biosynthesis of stilbenes is only possible in the presence of the so-called elicitor compounds, the most commonly used of which are cyclodextrins. We also report here on the induction of resveratrol production by cyclodextrins or combinatory elicitation in plant cell systems as well as the mechanisms by which they are able to trigger a stilbene response. The present article therefore discusses the role of cyclodextrins in stilbene chemistry both at the physico-chemical level as well as the biomedical and biotechnological levels, emphasizing the notion of "easy alliance" between these compounds and stilbenes.

Discovered in 1940 by Takaoka in the roots of the white hellebore and subsequently identified as a phytoalexin, that is, small biocidal molecules produced by plants as a response to stress, in grapevine [1] and peanut [2], resveratrol, which belongs to the rather restricted chemical group of stilbenes, has mainly been the focus of studies undertaken by the phytopathologists' community until the onset of the 90s [3–5]. At the time, work mainly targeted its biosynthetic pathway [6], antifungal activity [7] and metabolism *in planta* [8] as well as by fungi [9]. The first reports on the production of resveratrol by grape berries [10,11] quickly led to the detection of this compound in wine by Siemann and Creasy [12]. The originality of the seminal work of these two authors was to put in relation the already known properties of resveratrol in traditional Chinese and Japanese medicine [13] and the cardioprotective effects of a moderate consumption of a wine rich in polyphenols in a population subjected to a hyperlipidemic diet, the so called famous "French Paradox" [14]. These convergent studies between the concentration of resveratrol in wine and its possible beneficial effects on human health, has led to a real explosion of the research on this compound at the end of the 90s, an interest which has not been denied since. John Pezutto, whose team was the first to demonstrate the cancer chemoprotective activity of this compound even evoked the "phenomenon resveratrol" [15,16]. Resveratrol and its derivatives, the number of which now exceeds a thousand, have been the subject of relatively recent bibliographic reviews [5,17–19].

From a biological point of view, resveratrol exhibits a cytotoxic activity against many cancer cell lines as well as anti-inflammatory properties [20–23]. There is a certain amount of preclinical and clinical evidence of its efficacy in the treatment of cardiovascular disease [24] and of resveratrol action as a blood pressure lowering agent [25]. Resveratrol was also described as being able to play a protective role in case of neurodegenerative diseases such as Alzheimer, Huntington and Parkinson, through its antioxidant activity [26–28]. Resveratrol displays antifungal properties against phytopathogens [7,29] or fungi responsible for candidiasis in humans [30]. Finally, resveratrol and its derivatives have excellent cosmetic properties as whitening agents for the treatment of melanin skin spots [31,32]. One can therefore see without being exhaustive, that resveratrol and in general stilbenes, possess many biological activities. However, most of these properties are based on studies conducted *in vitro*. Several obstacles limit the study of the biological activity of resveratrol and its derivatives *in vivo*. The first one is the weak water-solubility of most stilbenes as well as their low bioavailability in humans and rats, as observed after oral administration; these features being quite common with polyphenols [33–35]. In addition, having these compounds in adequate quantities for the design of biological tests *in vivo* is hampered by the difficulty of obtaining them by pure chemical syntheses, which are time-consuming as well as environmentally unfriendly processes [36,37]. Bio-producing stilbenes by biological systems, mainly plant tissue cultures or cell suspensions in response to molecules capable of eliciting their synthesis, also provides an interesting alternative in terms of available quantities and green processes [38–40]. To address these fundamental questions, we show in this review how cyclodextrins, which are cyclic molecules built from a few glucose units, constitute valuable allies in the chemistry of stilbenes. The design of nanomolecular sponges using cyclodextrins capable of increasing the solubility, inclusion and delivery of stilbenes to their target cells is a first example. Use of cyclodextrins can also provide interesting applications in the green synthesis of stilbenes, particularly, for obtaining water-soluble glucosylated derivatives. Finally, the eliciting

properties of cyclodextrins on the biosynthesis of stilbenes, not only of monomeric stilbenes but also of oligomeric stilbenes, can be applied in plant biotechnology for the natural sourcing of these compounds.

Stilbene chemistry and biosynthesis: a condensed overview

Phytostilbenes are generally low molecular weight compounds varying from 212 Da for pinosylvin (3,4-dihydroxystilbene) or 228 Da for resveratrol (3,5,4'-trihydroxystilbene) (Fig. 1) and up to 1587 Da for pauciflorol D, a resveratrol heptamer identified in *Vatica pauciflora* [41]. All these compounds contain a 1,2-diphenylethylene ring based on the C6-C2-C6 backbone. The work of Stephenson's group has demonstrated very brilliantly that all stilbenes, comprising oligomers varying in number and structure, are derived from a single block, resveratrol, making this compound the iconic molecule of this group [19]. Resveratrol biosynthesis hails from the phenylpropanoid pathway, which is common to lignins and flavonoids [39,42] (Fig. 2). This pathway begins with the oxidative deamination of phenylalanine, an amino acid which drains 30% of all the carbon assimilated during photosynthesis [43]. This first reaction, catalyzed by phenylalanine ammonia lyase (PAL), leads to *para*-coumaric acid, the hydroxylation of which at position 4 is ensured by cinnamate-4-hydroxylase, an enzyme from the cytochrome P450 hydroxylase superfamily. In a secondary way, *para*-coumaric acid can be obtained directly from tyrosine *via* TAL (tyrosine ammonia lyase) (see [5] for a review). The final condensation between the *para*-coumaroyl-coenzyme A formed by ligation of *p*-coumarate with a coenzyme A (CoA) molecule *via* a CoA ligase and three malonyl-CoA units formed from the glycolysis-derived acetyl-CoA, is catalyzed by stilbene synthase during an iterative condensation process including the loss of four molecules of CO_2 [44,45].

Once the trihydroxystilbene skeleton of resveratrol is built, a high level of chemical diversification of stilbenes is then obtained thanks to various decorating enzymes like prenylases, hydroxylases as well as glucosyl and methyltransferases [5]. These enzymes lead to different monomeric stilbenes, some of which are described in this work: hydroxylated stilbenes, piceatannol and oxyresveratrol; methylated stilbenes, pterostilbene and glucosylated stilbenes, polydatin or piceid and 4'-β-*O*-D-glucosyl resveratrol (Fig. 1). On the other hand, the subsequent polymerization of resveratrol takes place through the action of plant peroxidases. The condensation of the phenoxyl radicals formed from resveratrol upon the action of peroxidases, does not take place in a randomized manner but in a defined order including various coupling modes [19]. Aside from their glucosylated derivatives, stilbenes, like many polyphenols, are poorly water-soluble compounds with low bioavailabilty [39,46].

Resveratrol solubility and bioavailability

While being less lipophilic than its demethylated derivative pterostilbene (Fig. 1), resveratrol is a hydrophobic compound as shown by a log P value of 3.0 to compare with that of methylated stilbenes (log P> 4) [47]. Due to its relative lipophilic character, resveratrol can easily cross membranes and seems to be well transferred in human bioengineered epithelia [48]. Although resveratrol displays promising and beneficial properties for human health, most of the data obtained stemmed from *in vitro* experiments carried out with cell cultures, tissues or bioengineered tissues [34]. The main

problem encountered with drugs displaying poor aqueous solubility is they cannot easily reach the target cells or tissues at sufficient concentrations to exert their action. *In vivo* studies of resveratrol bioactivity address questions regarding its absorption and bioavailability. Some key parameters commonly used in pharmacokinetics are the area under the curve, AUC, the maximal plasmatic concentration, C_{max} (and the maximal time t_{max} to reach C_{max}), half time value, $t_{1/2}$ and drug bioavailability, *F*. Mathematically, the AUC of a given drug corresponds to the sum of its instantaneous concentrations in the plasma for a given (0 to t) time interval. AUC is given by the following relation in case of a system with one compartment:

$$\mathrm{AUC}_0^{\mathrm{t}} = \int_0^{\mathrm{t}} \mathrm{C}_0 \, \mathrm{e}^{-\mathrm{kt}}$$

Here, C_0 is the initial drug concentration in the plasma and k is the elimination constant of the drug

The bioavailability of a drug is the fraction of the drug which reaches the systemic circulation when it is administered *via* non-intravenous routes as compared to the intravenous one. *F* can be calculated (in %) according to the formula given below with an orally administered drug:

$$F = \left[\frac{\mathrm{AUC_{OA}} \times \mathrm{dose_{IVA}}}{\mathrm{AUC_{IVA}} \times \mathrm{dose_{OA}}} \right] \times 100$$

Where AUC_{OA}= AUC oral administration; AUC_{IVA}, AUC intravenous administration; $dose_{IVA}$, drug dose via the intravenous route and $dose_{OA}$, drug dose *via* oral administration.

The pioneering studies of Goldberg et al. [49] and Walle et al. [35], respectively, have shown that upon oral administration of 25 mg doses of various wine polyphenols including resveratrol or the single oral administration of 25 mg radiolabelled resveratrol, this compound seemed to display an unusual high absorption rate (70%) at the gastro-intestinal tract (GIT) when addressing the sum of all its metabolites (both glucuronated and sulfated ones). However, Walle et al. [35] concluded that the bioavailability of *non-metabolized* resveratrol remains at a very low level of around 1%. In fact, resveratrol is rapidly transformed in the small intestine by enterocytes where it undergoes either glucuronidation or sulfation implicating glucuronidases [50,51] and sulfotransferases [50,52–54], a certain fraction of these sulfo- and glucurono-derivatives entering the portal circulation [50]. Some studies have reported moderate *F* values for resveratrol following oral administration as compared to intravenous dosing in rats: 38.8% [33,55] and 29.8% [33]. Surprisingly, the more hydrophobic and less polar pterostilbene (3,5-dimethoxy-resveratrol) was found to reach substantial *F* values, 12.5% [55] and 66.9% [33].

Preclinical and clinical experiments conducted in human groups after oral administration of resveratrol in the form of repeated doses ranging from 30 to 5000 mg per day, revealed varying but generally low resveratrol peak plasma concentrations (C_{max}): 0.56 - 2967.325 ng/mL [56–62], pterostilbene displaying higher total plasma levels (C_{max}: 2820-7880 ng/mL) [33]. All the afore-mentioned works underlined poor bioavailability of resveratrol after oral administration *via* single or

repeated dosing. Such limitations have thus opened the way for the search of alternative methods to increase resveratrol/derivative bioavailability. Some of them like the use of cyclodextrins as nanocarriers for the transport of resveratrol as well as utilization of cyclodextrins for the green synthesis of more polar and soluble resveratrol derivatives, are described in the following sections of this review.

Cyclodextrins as nanomolecular carriers and their use

Biological membranes represent a barrier for the penetration, delivery and therapeutic action of many drugs [63]. Targeted drug solubilizers for oral, transdermal, transmucosal or parenteral formulations are thus needed to overcome these limitations [64]. Drug vectorization has been achieved through use of various nanocarriers including liposomes, dendrimers and polymeric nanoparticles of range size from 1 to 1000 nm, namely for cancer treatment [65]. Among these, cyclodextrins have revealed very interesting properties as nano-vehicles for many drugs [63,66,67] as well as themselves displaying antiviral properties [68] and cytotoxic effects at high concentrations on diverse cancer cell lines [69]. Cyclodextrins have already been used as nanocarriers for established anticancer drugs like camptothecin (prostate cancer) [70], paclitaxel (ovarian, breast and lung cancers) [71], erlotinib (non-small cell lung cancer) [72] and tamoxifen (breast cancer) [73]. Cyclodextrins were also employed for the release of many other drugs, for example, anti-inflammatory drugs such as acetyl salicylic acid [74], oxaprozin [75], antivirals such as rilpivirine [76], the anti-HIV1 protease inhibitor lopinavir [77], antifungals like econazole [78] and antibacterial drugs such as norfloxacin [79]. Cyclodextrin-mediated drug delivery has been experimented in case of neurodegenerative diseases, as well. Molecularly-imprinted cyclodextrin nanoparticles have indeed been designed for the dihydroxyphenylalanine (DOPA)-prodrug delivery in the treatment of Parkinson's disease [80] as well as for facilitating the crossing of the blood-brain barrier of crocetin, a natural inhibitor of amyloid β plaque formation in the treatment of Alzheimer's disease [81] among other nanovectors used for anti-Alzheimer's drug delivery [82]. CDs are safe products approved by the Food and Drug Administration (FDA) [64]. CDs themselves do not display any biological activity unless employed at very high concentrations [69].

The French Chemist Villiers observed in 1891 that potato starch seeded with *Bacillus amylobacter* (*Clostridium butyricum*) yielded, besides dextrins, two carbohydrates forming "beautiful crystals" in low amounts, named cellulosines and which were attributed a multiple of the following formula $[(C_6H_{10}O_5)_2 + 3\ H_2O]$ [83]. A long time after, the two crystals obtained by Villiers were identified by Manor and Saenger [84] as being more likely α-cyclodextrin with the formula $[(C_6H_{10}O_5)_6.6H_2O]$ and β-cyclodextrin. Cyclodextrins form cyclic oligosaccharidic assemblies constituted of several α-1,4-linked glucopyranose units (hereafter named as glucose units). They are mainly composed of six (CD6) (α-cyclodextrins), seven (CD7) (β-cyclodextrins) and eight glucose units (CD8) (γ-cyclodextrins) [63,67]. This cyclic oligosaccharidic structure delimits at the supramolecular level a sort of truncated cone as imposed by the peculiar location of the primary hydroxyl groups of the α-D-glucopyranose units on one rim of the structure being the secondary hydroxyl groups on the other [85] (Fig. 3). Cyclodextrins thus comprise an inner hydrophobic cavity with the sugar hydroxyl groups being externally oriented [63]. Cyclic structures composed of a lower number of glucose units (< CD5) were not known and reputed not to allow stable conformations of glucose units until the recent work of

Yamada group demonstrating the feasibility of the synthesis of smaller cyclodextrins such as CD3 (three glucose units) and CD4 (four glucose units), which could be utilizable for the inclusion of therapeutic molecules of very small size [86].

Cyclodextrins not only improve the solubility and above all the bioavailability of hydrophobic compounds including both synthetic and natural drugs, they provide them with protection against numerous environmental conditions such as light, pH and temperature variations, oxidation and enzymatic degradation [63,66,87]. Internalization of drugs within cyclodextrins is related to the cyclodextrin cavity size including the inner and outer diameters which are on average the following: 57/137 nm, 78/153 nm and 95/169 for α-, β- and γ-cyclodextrins, respectively [64] (Fig. 3). Torus shape and opening of α-cyclodextrins are thought to be too tight to permit the formation of inclusion complexes with many drugs leading to the preferential use of β-cyclodextrins, even γ-cyclodextrins for high-molecular weight drugs [64]. However, measurement of the binding affinity energy of various cyclodextrins for resveratrol reported for example, very close values (-5.4 Kcal/mol and -5.3 Kcal/mol) for β- and γ-CDs, respectively [88].

As surprising as it may seem, β-cyclodextrins (CDs) possess an aqueous solubility (eight to twelve-fold lower) than the other two main cyclodextrin groups (α- and γ-CDs) [85,89–92], though they constitute the preferred CDs as drug carriers in many experiments for their low cost of production and cavity size best suited for numerous drugs [64]. The water solubility of β-CDs has thus been increased through chemical modifications of the glucose secondary hydroxyl groups. These include methylated β-CDs (mono-, di- and trimethylated CDs as well as randomized methylation of the cyclodextrin core), hydroxy-alkylated β-CDs (mainly hydroxypropyl-β-CDs, HP-β-CDs), various glucosyl-β-CDs (glucosyl-β-CDs, G1-β-CD and maltosyl-β-CDs, G2-β-CD) and sulfonic acid-β-CD derivatives (sulfobutylether-β-CDs) [63,64,66,67,85,93] (Fig. 4). Substituting groups may be chosen with a specific goal. Some studies have selected CD derivatives not subject to changes of the ionization state of the substituents in relation with pH variations. For instance, sulfobutylether CDs containing sulfonates or sulfates are stable in the anionic state at physiological pH [64]. CDs such as HP-β-CDs, have also been used in combination with biopolymer-liposomes [94,95]. All these types of CD have been employed for the vectorization of resveratrol and its derivatives (see next section).

Cyclodextrin chemistry has switched to other ways including the synthesis of hypercross-linked materials named CD-polymers when consisting of slightly condensed and water soluble cyclodextrins on one hand, or cyclodextrin-based nanosponges, which are highly polymerized and insoluble CDs, on the other. CDs of increased site specificity in drug delivery as a response to a given stimulus are termed stimuli-responsive CD nanosponges and have been developed more recently [96–99]. The three-dimensional mesh polymer network generated by the cross linking of the CD monomers thus forms nanocavities for various drug inclusion [77]. Cross linking may occur upon the condensation of CDs with reagents such as carboxylic acid dianhydrides (pyromellitic dianhydride) leading to carboxylate CDs [77,96], carbonyldiimidazole yielding carbonyl-CDs [97,98,100] (Fig. 5) or 1,6-diisocyanatohexane for the fabrication of polymerized CDs [88]. Condensation of two β-CDs with pyromellitic dianhydride yielded a CD polymer increasing by 12-14 fold the solubility of the anti-HIV1 drug, lopinavir [77].

To deliver drugs in a more specific way, a lot of stimuli-responsive nanosystems-based CDs were conceived [99,101]. Inclusion of photochromic moieties into nanocarriers generates light responsive systems whose light-induced modification can lead to conformational changes of the carrier and consequently to drug release [102,103]. Another option for modifying nanocarriers is the addition of ionizable groups such as carboxylates or amines to build pH-responsive drug transporters [104,105]. Differences in pH between tumor and inflammation tissue environments and normal healthy tissues, with the tumor microenvironment being more acidic than normal tissues [106], may justify the building of pH-responsive nanosponges for anticancer and anti-inflammatory drug delivery [104,107]. A similar reasoning applies to the synthesis of temperature-responsive nanosystems [108,109] which is based on the fact that hyperthermia is associated with pathological processes. Redox-responsive nanocarriers are particularly interesting to exploit the property of certain cancer tissues to contain significantly higher levels of glutathione (GSH) than normal ones, where these high GSH amounts are linked to tumoral progression and resistance to chemotherapy [110]. Disulfide bonds present in some redox-responsive nanocarriers are easily reduced by enzymes of the thioredoxin family localized in the cytoplasm, endoplasmic reticulum or even lysosomes in the presence of GSH [111]. Disulfide bond containing nanovehicles have thus appeared as particularly useful for site-specific drug delivery and, namely, for resveratrol [112,113] (Fig. 6).

Before focusing on resveratrol complexation with CDs, let us remember briefly that CD encapsulation has already been reported for many polyphenols [66]. In order to improve the water solubility, thermal stability, photostability as well as the bioavailability of these compounds, numerous works have described the synthesis of inclusion complexes between flavonoids and CDs, among others: β-CD–rutin complexes for increased antibacterial activity [114], β-CD–quercetin inclusion complexes for establishing potent nose-to-brain drug carriers [115], hydroxypropyl-β-CD encapsulation of naringenin for anti-inflammatory effects [116], daidzein and genistein inclusion complexes with hydroxypropyl- and sulfobutylether-β-CDs as part of a combined therapy for mucopolysaccharidosis [117], and curcumin crosslinked CD nanosponges for cancer treatment [118].

Physico-chemical aspects of resveratrol/stilbene complexation by cyclodextrins:

Formation of inclusion complexes between cyclodextrins and “guest” molecules is defined by two important physico-chemical parameters, the stoichiometry of the internalization process and the binding constant *K* between cyclodextrins and guest compounds, which are given by the following equations in case of a 1:1 stoichiometry [119]:

$$\mathrm{CD} + \mathrm{guest} \leftrightarrows \mathrm{CD:guest}$$

$$K = \frac{[\mathrm{CD:guest}]}{[\mathrm{CD}]\ \mathrm{x}\ [\mathrm{guest}]}$$

where [CD], [CD-guest] and [guest] are concentrations at the equilibrium.

A stoichiometry of 1:1 is corresponding to an inclusion formed by one cyclodextrin with one guest. The stoichiometry becomes 1:2 (or more) in case of a cyclodextrin fixing two (or more) guests and 2:1 for one guest molecule being complexed with two (or more) molecules of cyclodextrins [66]. A 1:1 stoichiometry in the CD inclusion complexes formed with resveratrol, pinosylvin, oxyresveratrol, piceatannol [120] or pterostilbene is generally the rule (see Table 1 and references therein), aside pinosylvin where a 1:2 stoichiometry is observed [121]. The stability or the complexation constant *K* (notated K_c or K_f) measures the strength of the association between the drug and the ligand. Otherwise speaking, K characterizes drug affinity for CDs [122]. The higher this constant, the higher the interaction between stilbenes and CDs [123]. Values of *K* differ according to the structure of the internalized stilbenes and the type of CDs being in the magnitude order of 10^2-10^4 M^{-1} (see Table 1 and references therein). The lowest K_c values recorded are 606.65 ± 30.18 M^{-1} for oxyresveratrol complexation on methyl-β-CDs [124] and the highest, 35864.72 ± 3415.89 M^{-1} for oxyresveratrol inclusion on hydroxypropyl-β-CDs [125]. According to some authors, high values of *K* may be detrimental to drug release from the inclusion complex [126,127]. Increase in the observed anticancer effects of resveratrol-loaded CDs was not found to be in line with the gain in resveratrol solubility observed upon resveratrol complexation with various CDs as compared to free resveratrol [97,99,127]. For example, around only 65% inhibition of cell viability on MCF-7 human breast cancer cells were recorded with 150 μM resveratrol + sulfobutylether- β-CD and 55% inhibition with free resveratrol despite an increased observed solubility of resveratrol of around 37-fold (0.03 mg/mL against 1.1 mg/mL). This was attributed to a high complexation constant *K* of 10,114 M^{-1} maybe explaining a higher retention of this compound [127]. Almost similar results were obtained regarding inhibition of a DU-145 prostate cell line:75% inhibition with a carbonyl-β-CD and 65% with resveratrol at 100 μM for a 3-fold enhanced solubility of resveratrol (0.04 mg/mL against 0.12 mg/mL) [97].

Among the various CDs available, the common ones, α-CD, β-CD and γ-CD have been used for resveratrol or derivatives complexation (Fig. 7) [93,119,123,125,128–132]. There are many studies reporting on the application of derivatized CDs to form inclusion complexes with resveratrol: hydroxypropyl-β-CDs (HP-β-CDs) [119,123–125,128–131,133–137], glucosylated-β–CDs like the maltosyl-β-CD (G2-β-CD) [138], methylated or ethylated-β-CDs such as monomethylated/ethylated-β-CDs [119,124,129,130,139], dimethylated-β-CDs (DIMEB) [123,128] and randomly-methylated-β-CDs (RAMEB) [140] (Table 1). As aforementioned, sulfobutylether β-CDs are well suited for both neutral and cationic substrates due to their stability in the anionic state at various pH values [64,127].

Finally, hypercross-linked CD nanosponges where the 3D mesh between CD units is established through carbonyl, carboxylate and disulfide bonds [97,99,100,141,142] or constituted of polymerized α-, β- and γ-CDs with 1,6-diisocyanotohexane [88], have been employed for resveratrol vectorization. In these intricated systems, resveratrol is internalized both in the inner cavities of CDs and the interstitial spaces managed between the cross-linked CDs thus increasing resveratrol loading efficiency [97] (Fig. 6). The most promising vectors for resveratrol are represented by the so-called bio-responsive nanosponges which constitute site-specific delivery systems for this compound [96–99,112].

Generally, resveratrol solubility increases in parallel with the resveratrol-CDs molar ratio, solubility being optimal for a resveratrol-CD ratio of 1:4 [134,142] (see Table 1). A solubility diagram of resveratrol recorded at pH 6 revealed an increasing solubility of this stilbene with increased CD

concentrations approaching a plateau at the 1:4 resveratrol-CD ratio [134]. Resveratrol solubility may also depend on chemical modification of CDs taking place on hydroxyl groups upon its complexation with CDs. Phase solubility diagrams showed an 8.5-fold increase in resveratrol solubility with β-CD and a 24-fold increased solubility with a HP-β-CD, these values almost doubling when the respective CD concentrations underwent a two-fold increase [143]. Stilbene or resveratrol complexation with CDs always leads to an increase in their water-solubility ranging from 2-fold [97] to the unbelievably high value of 700,000-fold recorded by Silva et al. [121] (Table 1). Resveratrol Inclusion complexes formed with γ-CDs were also reported as enhancing its solubility in lemon juices from 4.8% to 43.1%, *i.e.*, a 9-fold increase [135]. In some studies, a higher solubility of resveratrol [131] or polydatin [130] was observed with HP-β-CDs than with non-derivated β-CDs (Table 1).

Two parameters are particularly useful in drug nanoformulation: drug loading on- and drug release from the nanoparticles. These factors are essential for determining the efficiency of the drug delivery process. Resveratrol loading on nanoparticles which can be expressed as %, is the ratio between entrapped resveratrol and CD weight [99]. Its values vary from 4 to 7% in polymerized α, β and γ-CDs depending on the CD type [88], from 9.95 to 16.12% in GSH-responsive nanosponges as a function of the resveratrol/CD weight ratio [99] and from 30-40% in carbonyl nanosponges [100,141] to more than 90% in both carboxylate and carbonyl nanosponges [142] (Table 1). The notion of drug loading can also be extended to the determination of the drug encapsulation efficiency (%), which is defined as the ratio between entrapped resveratrol in CDs and total resveratrol concentration in the mobile phase [99]. The values of around 80% obtained for resveratrol and oxyresveratrol confirm a high encapsulation rate of stilbene compounds in nanosponges [97,99] though it can be lower (29%) [144]. Resveratrol loading efficiency is enhanced in conjunction with the stilbene-CD weight ratio of the inclusion complex [99,100]. Resveratrol loading passed from 9.95% to 16.12% on glutathione-responsive nanosponges for weight ratios of respectively 1:2 and 1:4 [99] and 11.93% (1:2 weight ratio) to 16.78% (1:6 weight ratio) for oxyresveratrol [97].

Release of resveratrol (or derivatives) from CDs or CD-nanosponges was expressed as the drug dissolution rate with time using the membrane diffusion method [97,99] or determined by measuring resveratrol release from resveratrol-loaded polymerized CDs in a liquid medium [88]. Release of resveratrol or oxyresveratrol from various CDs and CD-nanosponges increased by 2 to 8 fold at different timing (1, 3 or 24 h) compared to their dissolution rate in the free forms [97,99,123,142]. Resveratrol complexation with HP-β-CDs and its further inclusion into biopolymer-liposomes led to a 100% loading, a value superior to its incorporation to both the CD and the double layer of liposomes (94.4%), though the former complex allowed a two-fold increase in resveratrol delivery (Table 1) [94].

Pharmacokinetic profile of resveratrol formulated with cyclodextrins

There are numerous *in vitro* studies describing the characteristics of stilbene-CD inclusion complexes (Table 1), however works on the pharmacokinetic parameters of resveratrol complexed with CDs stemming from *in vivo* studies and following different modes of administration are less numerous [133,142,145] compared to flavonoids [146]. The seminal work of Das et al. [145] provided the first pharmacokinetic profiles regarding resveratrol-CD formulations. In this study, intravenous administration of resveratrol was carried out in rats with HP-β-CD while oral absorption of

resveratrol was performed using RAMEB-β-CD (randomly methylated-β-CD) and compared to a suspension of this compound in carboxymethylcellulose (CMC). Although resveratrol internalization with CDs increased its solubility by 59,500 fold, the $AUC_{0\rightarrow5h}$ (505.9 ng x h/mL) following resveratrol-HP-β-CD intravenous administration at a dosing of 10 mg/kg did not significantly differ from intravenous injection of the plain compound (10 mg/kg resveratrol in a sodium salt suspension) with an $AUC_{0\rightarrow5h}$ of 532.9 ng x h/mL. Oral formulation of resveratrol with RAMEB-β-CD at the dose of 50 mg/kg both increased C_{max} and t_{max} without significantly modifying $AUC_{0\rightarrow8h}$ (1009 ng x h/mL) nor resveratrol bioavailability (*F*=39.9%) as compared to the CMC resveratrol suspension ($AUC_{0\rightarrow8h}$= 981 ng x h/ mL; *F* = 38.8%) [145] (Table 2). However, using two sorts of resveratrol-CD nanosponges, one carbonyl nanosponge formed by crosslinking β-CD with diphenylcarbonate (R-NS I) and a carboxylate one fabricated from β-CD and pyromellitic dianhydride (R-NS II), a significant resveratrol loading efficiency of around 91% (Tables 1 and 2) was recorded in rats following a 20 mg/kg oral absorption of R-NS I and R-NS II compared to resveratrol alone as well as a two-fold increase in C_{max} and AUC values ($AUC_{0\rightarrow24h}$ 4145 and 3917 ng x h/ mL *vs* 2080 ng x h/ mL) [142] (Table 2).

In a comparative study performed in rats, pulmonary administration (orotracheal intubation) of resveratrol-HP-β-CD inclusion complexes in various dosages were evaluated against intravenous, intra-gastric and nasal inhalation administration [133]. Reported data showed better pharmacokinetic profiles (C_{max}, $AUC_{0\rightarrow10h}$, $AUC_{0\rightarrow\infty}$) according to the trans-pulmonary route *vs* all other routes with decreasing *F* values, 92.95% (pulmonary administration), 76.31% (nasal inhalation) and only 16.68% (intra-gastric route) (Table 2).

These studies therefore indicate that resveratrol bioavailability upon inclusion with cyclodextrins can be increased by a factor 2 when using CD-nanosponges compared to oral administration of the unloaded compound [142,145]. It also depends on its mode of administration [133].

Stilbene/cyclodextrin inclusions increase stilbene photostability

Generally, inclusion complexation of stilbenes with CDs or nanosponges has a positive effect on their photostability [97,121,123,125,130,134,142,147,148] and thermostability [125]. Light exposure can indeed be very detrimental to highly photosensitive compounds or drugs. Complexation with CDs has namely been described to delay photodegradation of the light versatile vasodilatator nifedipine [149]. It is well established that the natural isomer of resveratrol (and its derivatives) is the *trans* form which easily yields the *cis* isomer within a few minutes of UV or sunlight exposure [8,150]. Bertacche et al. [123] reported that only α-CD was efficient in protecting resveratrol from sunlight as compared to the larger β- and γ-CDs, though all CDs were found to confer resveratrol stability against UV radiations of 254 and 365 nm. It was suggested that the three-dimensional network constituted by CDs [134] or nanosponges [97,142] negatively affects light scattering due to a screening effect.

Reported benefits of stilbene/cyclodextrin inclusion complexes

All data tend to demonstrate that inclusion of resveratrol and its derivatives in CDs improves their solubility as well as their loading on-and release from CDs (Table 1 and references therein). Most of the experiments conducted *in vitro* or *in vivo* which have been put in place to validate the benefits of stilbene internalization in CDs on their biological activity, may principally resume in the

study of the antioxidant capabilities and cytotoxic actions of the complexes obtained. Besides, other works have reported the usefulness of stilbene inclusion with CDs for biomedical applications *in vivo* [88,132,151,152].

Antioxidant activity of stilbene-cyclodextrin inclusion complexes

The antioxidant activity of stilbene-CD inclusion complexes was mainly evaluated by their capacity to enhance scavenging of stable radicals such as $DPPH^{\cdot}$ [88,97,130,131,134,140], $ABTS^{+\cdot}$ and $SO^{+\cdot}$ [135] or the lipid peroxidation state [143]. There is converging evidence in some studies that internalization of stilbenes in CDs or nanosponges increases their antioxidant properties compared to the free compounds. For example, the reducing power of polydatin as determined with the Fe^{3+}/ferricyanide complex, as well as its $DPPH^{\cdot}$ radical scavenging activity were respectively enhanced by 2 and 1.5 fold upon inclusion with CDs, the best performances being observed with HP-β-CD [130] (Table 3). Dhakar et al. [97] reported a 75% $DPPH^{\cdot}$ radical inhibition activity with resveratrol-carbonyl-β-CD nanosponges *vs* 45% (1.7 fold-increase) with the plain compound at a 100 μM concentration. The same trend was also reported with oxyresveratrol-carbonyl-β-CD nanosponges at the 50 μM level. Supplementation of lemon juice with resveratrol-γ-CD complexes allowed to maintain juices' antioxidant capacity over 28 days compared to free resveratrol supplementation possibly leading to pertinent application to functional food [135]. In the same way, a strong inhibition of lipid peroxidation was described with resveratrol-CD complexes [143]. Haley et al. [88] showed in a pilot study, that localized resveratrol delivery performed with polymerized α-, β- and γ-CDs maintained a significant $DPPH^{\cdot}$ radical scavenging activity in the oxidative stress microenvironment generated by implanted intracortical microelectrodes, which are used in the treatment of several neurological disorders, thus increasing their operating time. This work adds value to the utilization of resveratrol inclusion CD complexes affording potential applications in neurology (Table 3).

At the opposite, no beneficial role of resveratrol encapsulation with CDs was demonstrated in other studies, its antioxidant capabilities being unchanged from resveratrol to resveratrol-CD complexes [131,134,140]. A strong interaction between CDs and stilbenes and possibly low drug release was reported as a plausible cause for the observed non-significant differences in the scavenging radical capacities of free resveratrol and its inclusion complex with methyl-β-CD despite increased resveratrol solubility and loading [140] (Tables 1 and 3). Here, a low enhancement (1.5-fold) in resveratrol release may account for this discrepancy [140].

Anticancer activity of stilbene-cyclodextrin inclusion complexes

All experimental studies conducted *in vitro* have shown a reduction of the cell viability of various malignant cell lines upon inclusion of resveratrol with CDs or nanosponge complexes *vs* free resveratrol (Table 3). For example, Pushpalatha et al. [142] noted IC_{50} values for the *in vitro* cytotoxicity of resveratrol carbonyl-β-CD or resveratrol carboxylate-β-CD nanosponges, 65% lower (IC_{50}= 110.70 μM and 117.34 μM) than those of the unloaded compound (IC_{50}=169.98 μM) on MCF-7 human breast cancer cells. A reduced IC_{50} value of 20 μM was observed upon resveratrol inclusion with HP-β-CD for inhibiting the proliferation of 7,12-dimethylbenz[a]anthracene-induced oral cancer cells

(HCPC-1 oral squamous cell carcinoma) compared to resveratrol alone (45 μM) [137]. Moreover, a spectacular regression of exophytic lesions displaying oral squamous cell carcinoma characters was recorded in hamster cheek pouches following topical applications of resveratrol-CD complexes *vs* free resveratrol [137]. A significantly higher inhibition of cell viability was also reported for oxyresveratrol (-75%) and resveratrol (-70%) loaded on carbonyl nanosponges at the 100 μM concentration on DU-145 prostate cancer cells compared to the free compounds (-60 and -50%, respectively) [97] (Table 3). At the same 100 μM concentration, a 1.5 fold-increase (40 to 60%), a 4 fold-increase (20 to 80%) and a 6 fold-increase (10 to 60%) were observed in the inhibition of cell viability (from unloaded resveratrol to resveratrol nanosponges) for one prostate cancer line (PC-3) and two colon cancer lines (HT-29 and HCT-116), respectively [141]. Reduction in the viability of HT-29 colon cancer cells also shifted from 15% with plain resveratrol to 40% with dual liposome-CD-resveratrol encapsulation complexes at a dose of 100 μM [94].

Very marked effects of resveratrol-HP-β-CD or resveratrol-β-CD complexations have been reported regarding the cell viability decrease of HeLa cervical carcinoma cells (-40%) and Hep3B hepatocellular liver cancer cells (-43 to -46%) compared to the only 5% recorded with unloaded resveratrol [143]. Extensive alterations of the cellular morphology including membrane collapse were also observed with CDs loaded with resveratrol though no such alterations were seen with free resveratrol [143]. Similar reduction of cell viability (> 90%) was reported upon resveratrol inclusion with other types of CDs such as RAMEB-β-CD *vs* resveratrol (70%) in Caco-2 human epithelial colorectal adenocarcinoma cells [140] or sulfobutylether-β-CDs (65%) in the MCF-7 breast cancer line than with resveratrol alone (55%) [127]. In this latter case, the slight difference observed in the reduction of the cell viability of those cancer cells was attributed to a high binding constant between resveratrol and CDs thus limiting resveratrol release efficiency. Resveratrol-sulfobutylether-β-CDs encapsulated in poly (lactic-co-glycolic acid) nanoparticles which have been proposed as an inhalable system for resveratrol delivery, displayed a remarkable inhibition of the cell viability of non-small cell lung cancer cells, reducing by respectively 15.39 and 50 fold the IC_{50} against the A549 and H358 cell lines compared to plain resveratrol [144].

Glutathione (GSH)-responsive nanosponges were used to selectively target cancer cells with elevated contents of GSH such as some ovarian and breast tumorigenic cell lines [99]. The 3-D mesh of these nanosponges is constituted by the CD cavities and the interstitial spaces managed by the cross linkage of the CDs with pyromellitic dianhydride and disulfure bridges (Fig. 6). The latter are lysed by endocellular enzymes of the thioredoxin family in the presence of high amounts of GSH thus facilitating release of resveratrol in the cell. Nanosponges are internalized in the cells through different endocytosis pathways [99]. At resveratrol concentrations from 100 to 200 μM, a 50-80% inhibition of the cell viability of the OVCAR3 ovarian cancer cell line and the MDAMB231 breast cancer cell line was reported with the resveratrol nanosponges, while a lower reduction in cell viability (-15%) was noted with the resveratrol nanosponges on normal human fibroblasts, the human mammary epithelial cell line MCF-10A or the SKOV3 human ovarian malignant cells, demonstrating the selective toxicity of these nanosponges [99].

Applications of stilbene-cyclodextrin inclusion complexes *in vivo*

Stilbene inclusions in CDs and their recognized benefits to increasing the solubility, release and bioavailability of these compounds have received some interesting applications in nanomedicine. For example, Vectisol® formulation of resveratrol, *i.e.* its encapsulation in a monopropane diamino-β-CD turned out to allow early recovery of proximal tubular function and glomerular filtration as well as a slowdown of loss of renal functions in a kidney transplantation preclinical study in pigs, thanks to resveratrol's antioxidant properties [132]. By reducing oxidative stress in the right ventricle of rats displaying monocrotaline-induced pulmonary hypertension in a *cor pulmonale* model, pterostilbene-HP-β-CDs inclusion ameliorates the systolic function of the ventricle as well as prevents it from structural alterations such as hypertrophy through an increase of pterostilbene bioavailability [151]. Likewise, pterostilbene encapsulation with HP-β-CDs was shown to preserve *via* a decrease of lipid peroxidation and the regulation of some antioxidant mechanisms, the function of the left ventricle following induced myocardial infarction in rats [152]. Additionally, inclusion of stilbenes in CDs may also have a positive effect by increasing their antimicrobial capabilities. These compounds are indeed known for possessing antifungal and antimicrobial activities [153]. Complexation of pterostilbene with HP-β-CDs, which is reputed to display higher fungitoxicity than its non-methylated counterpart resveratrol, was reported to diminish by 7.5 fold the minimum inhibiting concentration and by 4 folds the minimum bactericidal concentration on growth of *Fusobacterium nucleatum*, a bacterial pathogen associated with periodontitis, compared to unloaded pterostilbene dissolved in DMSO [136].

Numerous works have provided a large piece of evidence that stilbene compounds, mainly resveratrol [31,154–157] or pterostilbene [158] are efficient in preventing ultraviolet-B induced damages of skin, treating cutaneous herpes [159], psoriasis [160], modulating skin cancer mechanisms or improving melanoma treatment with potential applications in onco-dermatology. CDs have been shown to constitute interesting agents as good vehicles for stilbene delivery and for ensuring high levels of compound penetration as well as safety of the tissues for the treatment of skin or mucosal cancers [100,134,137]. Experiments with various matrices including rabbit mucosa [100], porcine skin [134] and porcine ear skin [161], revealed an increased *ex vivo* skin penetration of resveratrol with resveratrol CD or nanosponge formulations. Resveratrol-nanosponges accumulated at a two fold-higher rate (600 μg/cm^2) than the plain compound (300 μg/cm^2) in porcine ear skin [161]. A similar trend was reported with resveratrol-HP-β-CDs in porcine skin [134] and resveratrol-carbonyl nanosponges in rabbit mucosa [100].

Implication of cyclodextrins for the green synthesis of stilbene derivatives

Glucosylation of stilbene compounds not only increases their aqueous solubility for potential uses in cosmetic and onco-dermatology but substitution by a glucosyl group at the 4'-position of stilbenes also protects them from oxidation by polyphenol-oxidases such as tyrosinases [162]. A lot of stilbene β-D-glucosides have been identified so far in plants, namely the 3-*O*-β-D-glucosyl-resveratrol (piceid or polydatin), the 4'-*O*-β-D-glucosyl-resveratrol (resveratroloside) and the 4'-*O*-β-D-glucosyl-piceatannol (Fig. 1) [39]. Research has moved over the past few years toward the synthesis of their α-anomeric counterparts whose aqueous solubility and surfactant properties are superior [163–166].

The major drawback in the green synthesis of stilbene glucosides is the compatibility of the solvent employed for both the glucose acceptor (here the starting stilbenes) and the enzyme used for

glucosylation. For this reason, often times, a compromise between enzyme stability and stilbene solubility is necessary [39]. Making use of green solvents could be the right answer to this paradox. The green synthesis of 3-*O*-α-D-glucosyl resveratrol with sucrose and not CDs as a glucose donor, has already been performed by a combination of an ionic liquid and a buffer, which considerably increases resveratrol solubility under the catalytic action of a phosphorylase from *Bifidobacterium adolescentis* [167]. Several works have reported achievement of stilbene *O*-glucosylation with cyclodextrin glucosyl- (glucano)-transferases (CGTases) from various sources as biocatalysts utilizing starch or CDs as glucose donors [163–166,168,169] (Table 4). CGTases have often been employed for the biosynthesis of various polyphenolic glucoside derivatives: epicatechin glucosides [170], kaempferol glucoside [171], genistein diglucoside [172], flavonol and flavanones glucosides [173], pinoresinol glucoside [174] or α-arbutin [175]. Torres et al. [169] have reported the use of a monophasic solvent system constituted of a mixture of one organic solvent (DMSO) and acetate buffer for the synthesis of a series of glucoside derivatives of resveratrol. In this synthesis, starch was employed as the primary glucose donor, glucosylation being ensured by the CD-glucanotransferases of *Thermoanaerobacter* or *Bacillus macerens*. Under these conditions, various glucoside derivatives of resveratrol were obtained with quite good 50% glucosylation yield, suggesting that CDs arising from the partially hydrolyzed starch were directly implicated in the transfer of the glucosyl moiety to stilbene acceptors. In a similar manner, the enzymatic production of a 4'-*O*-α-glucoside of pterostilbene whose solubility is lower than that of hydroxystilbenes, was described in a monophasic solvent system constituted by DMSO and buffer with the CGTase of *Thermoanaerobacter* and starch as the primary source for glucosyl groups [163]. However, the high proportion of DMSO in the solvent mixture renders this synthetic route unsuitable for the green production of stilbene glucosides.

As aforementioned, CDs allow the increasing of the internalization rate of compounds poorly soluble in water such as stilbene aglycones. Their use is thus particularly conducive to the green synthesis of stilbene glucoside derivatives [39,164,165]. The transfer of an α-glucoside group or more groups from the donor (the cyclodextrin) to the acceptor (the stilbene) may proceed through coupling of the cyclodextrin and the stilbene, which randomly attach to the active site of the CGTase [168,176]. A plausible mechanism for the formation of a series of piceid (referred as $picG_1$) derivatives considerably varying in the number of the glucosyl groups has been deciphered under the action of the CGTase of *B. macerans* [168] (Fig. 8). A primary nucleophilic attack of the 4'-hydroxyphenyl group of piceid ($picG_1$) on the Carbon 1 at the reducing end of an opened α-CD, maltohexaose, results in an α-(1,4) linkage between piceid and the maltohexaose leading to the release of an initial coupling product called $picG_7$. Following the disproportionation reaction of $picG_7$, various glucoside derivatives of $picG_1$ like $picG_2$, $picG_3$, etc. are then otained [168]. This mechanism may explain not only the recovery of monoglucosides but also of di and tri-glucosides during the glucosylation experiments of resveratrol in presence of CGTases (see below) [164,165,169]. Polyglucosylated derivatives of 4'-*O*-β-resveratrol-glucoside like 4'-*O*-β-maltoside, 4'-*O*-β-maltotrioside, 4'-*O*-β-maltotetraoside and 4'-*O*-β-maltopentaoside acting as potent inhibitors of phosphodiesterase activity and displaying possible neuroprotective properties, were obtained through a synthetic route including α-CD and a plant CGTase in a medium totally free from organic solvent [166]. One may pay attention to the fact that in

this case, only the β-anomeric forms were obtained instead of the commonly recovered α-glucosides (Table 4).

The CGTase-catalyzed synthesis of hundred milligrams of α-*O*-D- mono and diglucosides of resveratrol (3 and 4'-α-*O*-D-glucosyl resveratrol as well as 3 and 4'-α-*O*-D-maltosyl resveratrol) was performed more recently at the 2-L bioreactor scale in water (MES buffer) with the CGTase from *Thermoanaerobacter* sp. (*Toruzyme*) and β-CD as a glucose donor [164] (Fig. 9). Maximization of the glucosylation transfer was achieved *via* the optimization of multiple factors such as pH, temperature, enzyme and donor amount as well as the resveratrol:CD ratio, performing a 35% yield based on molar concentrations. This yield increases up to 50% when a 1 kDa cut-off membrane is coupled to the enzymatic reactor thus allowing retention of the resveratrol β-CD inclusion complex in the medium and increasing the transfer rate of the glucoside derivatives formed in the permeate such that they are protected from further hydrolysis [165]. The production rates of the 3 and the 4'-*O*-α-glucosides of resveratrol were almost similar indicating the absence of any regioselectivity in the glucosylation process implicating CGTase on the stilbene moiety [164] (Table 4).

Glucosylation of stilbenes renders them more soluble in water making them utilizable for topical applications in case of cutaneous disorders in cosmetics and onco-dermatology [177]. Torres et al. [169] indeed noted a 67-fold increase in the solubility of resveratrol-α-glucosides compared to resveratrol. Likewise, pterostilbene, which is an almost insoluble compound in water, has its solubility reaching 0.1 g per liter upon glucosylation [163]. Except the study of Shimoda et al. [166] reporting an increase in the inhibition of phosphodiesterase activity with resveratrol glucosides that suggests their potential for the treatment of neurodegenerative diseases, other works conducted on the biological activity of stilbene glucosides tend to show paradoxically a decrease in their antioxidant and cytotoxic effects with regards to the aglycones. By taking resveratrol as the reference compound with an antioxidant activity of 100%, the relative activities of the 3 and the 4'-*O*-α-glucosides of resveratrol were respectively of only 40 and 70% [164,169] as confirmation that glucosylation on the 4'-position of stilbenes is less detrimental to their biological activity [162]. Similarly, Gonzalez-Alfonso et al. [163] reported a near 40% decrease in the antioxidant activity of 4'-*O*-α-glucoside of pterostilbene as well as a significantly lower toxicity on HT-29 colon cancer cells compared to the aglycone.

Apart from the synthesis of stilbene glucosides, use of RAMEB-β–CDs was also found to facilitate hydroxylation of the stilbene core with engineered cytochrome P450 leading to various di- and trihydroxystilbenes and limiting the use of organic solvents to a few percent [178].

Cyclodextrins for the induction of stilbene production in plant cell systems

As aforementioned, one major feature of CDs is their ability to form inclusion complexes with poor water-soluble organic molecules due to the hydrophobic character of their central cavity, which thus serve as nano-sized carriers for these molecules in aqueous solutions. In addition to such a remarkable property, CDs are able to interact with plant cells in which they can trigger a cellular response. This makes them useful tools to study plant biochemistry and physiology as well as biotechnology aspects. The first evidence for a CD-plant cell interaction arose from experiments run with grapevine cell cultures treated with the phytoalexin resveratrol, either unloaded or complexed

with the dimethyl-β-CD (DM-β-CD) in order to evaluate its efficacy as a protecting agent against the phytopathogen *Xylophylus ampelinus*. Although unloaded resveratrol completely disappeared within 48 h, resveratrol loaded on DM-β-CD remained stable in the medium. Unexpectedly, controls treated only with DM-β-CD exhibited an accumulation of resveratrol evidencing for the first time that CDs may act as inducers of *de novo* resveratrol synthesis in grapevine cells [179].

As seen before, CDs display a high chemical diversity, including CDs of natural origin with free hydroxyl groups, and the ones of synthetic origin, with chemical groups attached to the glucosidic OH groups [63]. The capability of a limited number of β-CDs to induce resveratrol bioproduction was first evaluated in grapevine cell cultures [180,181]. Only chemically modified CDs, *e.g.* methyl-or hydroxypropyl-CDs, induced a strong resveratrol production unlike natural CDs, which yielded a very weak response. However, sulfated β-CDs, which are frequently used as carriers in pharmaceutical formulations [64], brought about a hypersensitive response in grapevine cells. Bru group's study thus highlighted the importance of the chemical nature of CD-linked groups to raise a cell response and suggested that one plausible reason for the reported elicitor activity of CDs is their structural similarity to the oligosaccharidic elicitors released from plant cell walls upon plant-fungal interactions. Dimethylated-β-CDs also well-known as DIMEB thus became the gold standard in subsequent research works. Another piece of evidence that CDs differentially interact with plant cells is the species- and genotype-dependent cell resveratrol production observed as a response to a particular cyclodextrin type [182].

CDs are almost non-toxic for cell cultures and display a superior eliciting activity than other oligosaccharides like chitosan, a major component of fungal cell walls [183]. Among the elicitors used to induce stilbene biosynthesis by plant cell or tissue systems, CDs lead to the highest production yields (in the g/L range) [180,181,184] compared to other common eliciting molecules derived from jasmonate, like methyljasmonate (MeJA) with reported production levels of only milligrams per liter [185–187]. Further works have shown empirically that combinatory elicitation with CDs and MeJA and, to a lesser extent, CDs plus coronatine, the jasmonate-Ile analog, synergize the effects of each elicitor increasing the production of resveratrol by 5 to 8-fold in grapevine cell suspensions [188–191]. Spectroscopic approaches for understanding the synergistic mechanisms existing between CDs and MeJA have reported that resveratrol, CDs and MeJA together in solution formed binary complexes, respectively CD-resveratrol and CD-MeJA but no ternary inclusion complexes [191]. CDs were demonstrated to improve the aqueous solubility of the reputed hydrophobic molecule, MeJA, resulting in an increase of resveratrol production by grapevine cells.

Cost is a key issue in biotechnology and the utilization of elicitors like DIMEB and coronatine could turn out to be quite expensive for large scale applications in bioreactors. Attempts to reduce the production costs incurred by CDs have led to a new strategy, such as using CD polymers coated with magnetic nanoparticles for the easy recover and reuse of the elicitor in plant cell cultures for optimizing resveratrol production [192]. The obtained results are promising as HP-β-CD coated polymers can be reused up to three times yielding resveratrol levels ranging from 0.3 and 0.5 g/L.

Stilbene production based on the utilization of CDs has also been accomplished in plant tissue systems like the hairy roots of *Arachis hypogaea*, *Vitis rotundifolia* and *V. vinifera* leading to the accumulation of tens of mg/g dry weight (DW) of resveratrol, piceid and resveratrol dimers in the

elicited tissues of grapevine or peanut [193–195]. Elicitation resulted in a successful strategy to both enhance the production level of those stilbenes and promote their extracellular accumulation, which is particularly useful for facilitating their extraction from the culture medium. Use of DIMEB was also reported to induce the production as well as modifying the profiles of some isoprenylated stilbenes belonging to the arachidin family (Fig. 1) in the hairy roots of *A. Hypogaea* [196,197].

Once the feasibility of producing a natural compound or drug by tissue or cell cultures has been demonstrated, the problem arises of transferring the results obtained, from the laboratory scale to the industrial production in bioreactors [32,38,198]. The high stilbene levels recovered in plant cell systems as a response to elicitation with CDs, particularly in grapevine cell cultures, have led to scale up the cultures from shaken flasks to bioreactors. Most grapevine cell cultures well tolerate the typical shear stress of the bioreactor environment, even with a stirred tank [184,199–201], although some genotypes seem to be more sensitive [183,202]. Both bubble column [201] and disposable bag wave bioreactors [203] are suitable for this purpose. Elicitation of stilbene production with DM-β-CD was successfully performed in bioreactors using the *V. vinifera* and *V. labrusca* cell lines. Recovered stilbene amounts well correlated with the respective achievements in shaken flasks though being slightly higher in bioreactors, most likely due to a better mass transfer. When using DM-β-CD alone, accomplished resveratrol yields were 2.2 and 3 mg/g fresh weight (FW) for *V. vinifera* cv Gamay cultures in V-shaped bubble columns and in stirred tank bioreactors, respectively. Resveratrol amounts rose to 13.5 mg/g $^{-1}$ FW in each bioreactor [201] and even reached 14.3 mg/g FW in a 20-litre stirred tank bioreactor upon combined elicitation with DM-β-CD and MeJA [200], which further confirms the synergistic effect already mentioned in shaken flasks [190].

Elicitation with cyclodextrins combined with plant metabolic engineering has been disclosed as a successful strategy to diversify the profile of stilbenes and other specialized metabolites produced by cell suspension cultures. For instance, grapevine cells transformed with the *human hydroxylase CYP1B1* [40] or the *Rosa hybrida orcinol*-O-*methyltransferase* [204] produced significant levels of resveratrol derivatives like piceatannol and pterostilbene, respectively, in addition to resveratrol upon elicitation. Likewise, the transformation of *Sylibum marianum* cultures with the *grapevine stilbene synthase 3* yielded 12 mg/L resveratrol upon elicitation with DM-β-CD, in addition to the accumulation of silymarin and coniferyl alcohol as in the wild lines [205].

Mechanisms of induction of stilbene production by cyclodextrins

Although CDs, and particularly DM-β-CDs, are known to induce a phytoalexin response in grapevine cells ending up in both the production and the extracellular accumulation of various stilbenes, the understanding of the cellular and molecular mechanisms involved in this response is far from being elucidated. Such events obviously include perception of CDs or their hydrolyzing products at the membrane level and induction of the related signaling pathways, followed by regulation of the key enzymes of stilbene biosynthesis, gene transcription changes as well as modifications of some membrane transporters. The mechanisms by which CDs are able to trigger the production of resveratrol and related stilbenes in the cell remain unexplained. A good comparison can be drawn with the induction of a phytoalexin response in soybean cotyledons by middle-chain oligogalacturonides released from the plant cell wall by fungal endo-polygalacturonases [206]. It is likely

that opening of the CD ring and subsequent hydrolysis of the glucosidic chain may also generate oligosaccharides with potent eliciting activities on resveratrol biosynthesis.

In order to decipher the early signaling events taking place during resveratrol biosynthesis induction in the presence of DM-β-CD or DM-β-CD + MeJA, the effect of blockers of extracellular Ca^{+2} fluxes, inhibitors of MAP kinases, NADPH oxidases and Tyr phosphatases as well as NO scavengers was studied in grapevine cell suspensions [207]. DM-β-CD / MeJA combination turned out to relieve the action of blockers of extracellular Ca^{+2} fluxes, MAPKs inhibitors and NO/H_2O_2 scavengers indicating that Ca^{2+} mobilization, NO and H_2O_2 production, MAP kinases and phosphatases are involved in the early signalization to reach resveratrol production (Fig. 10) [207]. Remarkably, these effects on signaling pathways resemble those reported for grapevine cell cultures treated with the microbial protein elicitor PG1 [208,209].

Transcription factors are major components in the regulation of cellular metabolic events fine-tuning the control of numerous biosynthetic routes including the resveratrol one comprising for example, the *Vitis vinifera* transcription factors VvWRKY24 and VvMyB14 being able to up-regulate *STS* gene expression on one hand, and the negative regulator VvWRKY8 of *STS* gene expression on the other (Fig. 10) [210–214]. Transcription factors like MYB15 which activates the transcription of stilbene synthase (STS) [215] and the NAC-type which promotes the biosynthesis of phenylpropanoids and monolignols [216], are up-regulated by DM-β-CD and further enhanced by DM-β-CD+MeJA (Fig. 10) [217]. Numerous biosynthetic enzymes from the connected pathways of shikimate, phenylalanine, phenylpropanoid (PAL, C4H, 4CL), malonyl CoA and stilbene (STS) biosynthesis are up-regulated by DM-β-CD, and DM-β-CD+MeJA to allow a marked carbon flow toward resveratrol biosynthesis [217]. Omics analyses conducted on grapevine cell cultures offered an overall picture of the major metabolic events following combined DM-β-CD and MeJA elicitation [217–219]. Proteomic changes strongly correlate with transcriptional events, particularly during changes in the activity of the enzymes catalyzing the late resveratrol biosynthesis steps (PAL, STS) [219]. Taken altogether, it would seem that CDs and combinatory elicitation with CDs and MeJA orchestrate resveratrol accumulation by two strategic actions: (i) activation of *STS* genes transcription; (ii) increase of the precursor supply taking into account that all the precursors of resveratrol biosynthesis are also shared by major competing pathways; *i.e.* monolignol and flavonoid routes. These omic studies also revealed the co-expression of certain glutathione-*S*-transferase isoforms at both the transcript and protein levels. Interestingly, overexpression of a tau class glutathione-*S*-transferase (VvGST U10a) possibly implicated in the transport of resveratrol was observed in grapevine cells upon elicitation with DM-β-CD or DM-β-CD+MeJA [218]. In peanut hairy roots, combinatory elicitation with DIMEB and MeJA also leads to the up-regulation of stilbene dimethylallyltransferases, which are implicated in the transfer of a dimethylallyl pyrophosphate group to various stilbenic compounds, in addition to STS [220]. This confirms the accumulation of prenylated stilbenes at levels similar with those of resveratrol (Fig. 1) [196]. Combinatory elicitation is thus also able to activate metabolic steps downstream resveratrol biosynthesis to diversify stilbene profiles.

Conclusions and future prospects

The involvement of CDs in the chemistry of resveratrol at both the physico-chemical level as well as the biomedical and biotechnological levels, was underlined in this work. Cyclodextrins can serve as nanomolecular-scale transporters for stilbenes to improve their solubility and bioavailability,

thereby ensuring their delivery at the cellular level. Inclusion of resveratrol and stilbenes in cyclodextrins increases their water solubility by a factor of 10 up to 10,000 depending on the studies, allowing them to be used in green chemistry particularly for the synthesis of glucosylated derivatives without the need for organic solvents. Finally, the reported eliciting properties of CDs on the production of stilbenes by tissue or cell cultures in quantities of the order of a few grams, constitutes a third aspect of what we have defined as the easy alliance between stilbenes and cyclodextrins.

As regard the nano-transport of resveratrol and its derivatives, it has generally been shown that CDs improve both their solubility in water and their bioavailability in animal models and, consequently, their anticancer and antioxidant activity as well as their biological properties during experiments carried out *in vivo*, compared to unloaded resveratrol. However, even if the percentage of resveratrol loaded on CDs is elevated, its release from CDs may be hampered in case of high resveratrol-CD association constants. Some authors have indeed suggested that the lack of differences recorded in the biological activity between free and CD-encapsulated resveratrol could be linked to high values of this constant. Regarding bioavailability, it seems that resveratrol inclusion with CDs modifies this parameter increasing it by a factor two when using CD-nanosponges, and a significant improvement in bioavailability was recorded depending on its mode of administration (pulmonary, nasal or intra-gastric) [133,142,145]. Further studies are thus needed to study the pharmacokinetic profiles of stilbenes *in vivo* upon nano-encapsulation with CDs.

Stilbene vectorization using CDs is now moving towards the production of more specific systems such as bioresponsive-cyclodextrin nanosponges targeting particular cell types or microenvironments. Trotta's group recently described the inexpensive synthesis of a GSH-responsive CD nanosponge capable of selectively targeting certain types of cancer cells. The crosslinking in this nanosystem contains disulfide bridges whose lysis in the presence of endogenous GSH and endocellular enzymes facilitates drug release. These nanosponges have successfully been studied using the anticancer drug, doxorubicin during *in vitro* experiments [112]. The method was transposed very recently to the design of GSH-bioresponsive nanosponges dedicated to the transport of resveratrol [99]. This type of resveratrol-nanosponges preferentially targets certain models of cancer cells *in vitro* (ovarian, breast and lung cancer cells), which contain higher levels of GSH than other cancer cell types and normal cells. GSH-responsive nanoparticles transporting resveratrol would therefore have to be further tested *in vivo* for the treatment of specific tumors and the modulation of tumor extracellular matrices in relation to the high GSH levels released by tumor-associated fibroblasts [99].

Use of CDs for the green synthesis of glucosylated derivatives of resveratrol and its derivatives has a double benefit, CDs both serve as donors of glucosyl moieties during the complex reactions of transglucosylation in the presence of CGTases and allow the solubilization of these compounds in water and buffer solutions [164–166] or limit to small amounts the incorporation of organic solvents [163,168]. Quantities of the order of a few hundred milligrams of resveratrol α-glucosides have been obtained from only 2 g of resveratrol in presence of a β-CD in 2 L-reactors, thus paving the way towards the application to syntheses on a larger scale [164]. Coupling the enzymatic reactors with membranes with a cut-off threshold of 1 kDa already makes it possible to optimize the accomplished yields [165].

Unexpectedly, CDs were reported the ability of inducing the production of resveratrol at the gram scale as well as yielding various profiles of stilbenes including hydroxylated, isoprenylated, glucosylated, methylated and oligomeric forms in plant cell or tissue systems. Research in this area will face two challenges: up-scaling the bioproduction of stilbenes at the industrial level and deciphering the mechanisms at the basis of their biosynthesis by plant cells and tissues. There are indeed still many knowledge gaps to bridge in the mechanisms by which CDs elicit resveratrol production in grapevine and other plant culture systems. All this requires further efforts, such as the discovery of receptor- and signaling cascade-specific proteins, additional transcriptional regulation players as well as membrane transporters enabling extracellular accumulation of stilbenes. It would be interesting to carry out a targeted gene expression analysis to explore whether MYB and WRKY transcription factors do respond or not to CD elicitation or combinatory elicitation with MeJA, and which *STS* paralogs are activated to obtain a more complete picture of the regulatory stilbene biosynthesis network in grapevine.

Legends of the figures:

Figure 1: Biosynthesis of stilbenes starting from phenylalanine and the alternative route from tyrosine. Abbreviations used: PAL, phenylalanine ammonia lyase; TAL, tyrosine ammonia lyase; C4H, cinnamate-4-hydroxylase; 4CL, 4-cinammoyl-CoA ligase; STS, stilbene synthase; CHS, chalcone synthase; ROMT, resveratrol-*O*-methyltransferase; GT, glucosyltransferases; UDPG, UDP-Glucose; PER, peroxidases

Figure 2: Chemical structures of some stilbene monomers described in this study. Hydroxystilbenes, resveratrol, piceatannol, oxyresveratrol and pinosylvin; stilbene glucosides, piceid, 4'-*O*-β-glucosyl-resveratrol (resveratroloside); methylated stilbenes, pterostilbene; isoprenylated stilbenes; arachidin-1, arachidin-2 and arachidin-3

Figure 3: Schematic representation of the truncated cones formed by the cyclic oligosaccharides of α-(CD6), β-(CD7) and γ-cyclodextrins (CD8). The cyclic oligosaccharidic assembly delimits at the supramolecular level a sort of truncated cone whose inner diameters are increasing according to the CD type.

Figure 4: Simplified structures of some derivated β-cyclodextrins. **1**; R = H, β-cyclodextrin, R= $-CH_2-CH[OH]-CH_3$, 2-hydroxypropyl-β-cyclodextrin; **2**, R= $-CH_3$, methyl-β-cyclodextrin; **3**, **3a**, R= $-SO_3Na$, β-cyclodextrin sulfate, **3b**, R= $-[CH_2]_4-SO_3Na$, sulfobutylether-β-cyclodextrin.

Figure 5: 3D representation of a carbonyl CD nanosponge. This type of nanosponge is obtained by reaction of a β-CD with carbonyldiimidazole yielding the carbonyl CD nanosponge and imidazole. Linking carbonyl groups are colored in red and blue

Figure 6: 3D representation of a GSH-responsive CD nanosponge. β-cyclodextrin cycles made of seven α-D-glucose units are linked with the crosslinker pyromellitic dianhydride and ethyldisulfide bridges. Diethylsulfide bridges are colored in yellow, oxygen atoms in red and hydrogen bonds in white.

Figure 7: Inclusion of resveratrol within the cavity of a β–cyclodextrin (realized by molecular docking)

Figure 8: Hypothetical mechanism of the formation of stilbene glucosides from cyclodextrins. Cleavage of the cycle of the α-cyclodextrin yields an opened α-cyclodextrin named maltohexaose. A primary nucleophilic attack of the hydroxyl situated at the 4'-position of piceid on the C1 at the reducing end of maltohexaose leads to an intermediate compound whose disproportionation leads to various piceid glucoside derivatives

Figure 9: Green synthesis of various *O*-α-glucosylated derivatives starting from β-cyclodextrin as a glucose donor. **A**, General scheme of the synthesis; **B**, schematic representation of resveratrol inclusion inside the β-cyclodextrin cavity. **1** and **2**, 3 and 4'-α-*O*-D-glucosyl resveratrol; **3** and **4**, 3 and 4'-α-*O*-D-maltosyl resveratrol. Abbreviations: R, resveratrol; β-CD, β-cyclodextrin; CGTase, cyclodextrin glucanotransferase

Figure 10: Regulation of stilbene biosynthesis through combinatory elicitation with dimethyl-β-CD (DIMEB) and MeJA elicitors in grapevine cells. Stilbene biosynthesis involves the production of the early precursors erythrose 4-P (E4P) and phosphenolpyruvate (PEP) from a carbon source through central carbohydrate pathways. The two direct precursors of resveratrol are produced through two diferent pathways: *p-coumaroyl CoA* is a final product of the two early precursors processed *via* the shikimate/aromatic aminoacid biosynthesis/phenylpropanoid serial pathways, and *Malonyl CoA* comes from a parallel processing of PEP through three enzymatic steps. The first stilbene, resveratrol, may undergo derivatization reactions out of which only two have been well characterized to date: methylation by resveratrol-*O*-methyltransferases in grapevine (VvROMT), and prenylation by resveratrol dimethylallyl transferases in peanut (AhR4/3'DT). Resveratrol and prenylated derivatives are found in the extracelular médium, as well. In grapevine cell cultures upon elicitation with DIMEB and DIMEB + MeJA, a tau class glutathione *S*-transferase (VvGSTU2) is putatively involved in the extracelular accumulation of resveratrol as free form or complexed with CDs. Elicitors such as DIMEB and MeJA trigger early signaling events starting from Ca^{+2} income from the apoplastic space that ends up in transcriptional regulation through a only partly established pathway where production of NO, H_2O_2 and participation of protein tyrosine phosphatases (TyrPase) and MAPK is involved. In *Vitis quinquangularis,* a MAPKKK38 transcription factor has been described to enhance the trancription of *STS* genes likely *via* the transcriptional activation of MYB14. In *V. amurensis,* Ca-dependent protein kinases activate the transcription of specific *STS* paralogs. In *V. vinífera,* the best characterized transcriptional activators of *STS* genes are MYB14/15 TFs, that are also able to activate the transcription of shikimate pathway key genes as well as those of *PAL* and *ROMT*. MYB14, WRKY8 and resveratrol are components of a regulatory loop in which MYB14 promotes the production of resveratrol; resveratrol activates the transcription of WRKY8, likely through undisclosed effector proteins, and WRKY8 interacts with MYB14 to block it, thus down-regulating resveratrol levels. Such a negative loop was discovered upon UV light irradiation which activates the transcription of MYB14. Other steps of the phenylpropanoid pathway have also specific transcriptional activators such as WRKY2 and MYB5a, and NAC TFs which are active up-regulators of some key steps of the shikimate pathway. Regulatory entities described in relation with combinatory elicitation with DIMEB and MeJA are shown in orange colour. Blue arrows indicate possible hierarchy between early signaling events. Green and red arrows stand for transcriptional up- and down-regulation respectively; solid lines indicate that the evidence has been validated in targeted experiments while slashed lines means the evidence only comes from omics analysis. Genes encoding for TFs have been labelled in their promoter regions according to the stimulus they respond: elicitor responding (ERE), hormone responding (HRE), UV light responding (UVRE) and resveratrol responding (RRE). DIMEB are symbolized by small troncated structures

894
895
896

References

1. Langcake, P. & Pryce, R. J. The production of resveratrol by Vitis vinifera and other members of the Vitaceae as a response to infection or injury. *Physiol. Plant Pathol.* **9**, 77–86 (1976).
2. Ingham, J. L. 3,5,4'-trihydroxystilbene as a phytoalexin from groundnuts (Arachis hypogaea). *Phytochemistry* **15**, 1791–1793 (1976).
3. Jeandet, P. *et al.* Phytoalexins from the vitaceae: Biosynthesis, phytoalexin gene expression in transgenic plants, antifungal activity, and metabolism. *J. Agric. Food Chem.* **50**, 2731–2741 (2002).
4. Jeandet, P. *et al.* Biosynthesis, metabolism, molecular engineering, and biological functions of stilbene phytoalexins in plants. *BioFactors* **36**, 331–341 (2010).
5. Jeandet, P. *et al.* Phytostilbenes as agrochemicals: biosynthesis, bioactivity, metabolic engineering and biotechnology. *Nat. Prod. Rep.* (2021) doi:10.1039/d0np00030b.
6. Langcake, P. & Pryce, R. J. The production of resveratrol and the viniferins by grapevines in response to ultraviolet irradiation. *Phytochemistry* **16**, 1193–1196 (1977).
7. Adrian, M., Jeandet, P., Veneau, J., Weston, L. A. & Bessis, R. Biological activity of resveratrol, a stilbenic compound from grapevines, against Botrytis cinerea, the causal agent for gray mold. *J. Chem. Ecol.* **23**, 1689–1702 (1997).
8. Jeandet, P. *et al.* HPLC analysis of grapevine phytoalexins coupling photodiode array detection and fluorometry. *Anal. Chem.* **69**, 5172–5177 (1997).
9. Breuil, A. C. *et al.* Metabolism of stilbene phytoalexins by botrytis cinerea: 1. Characterization of a resveratrol dehydrodimer. *Tetrahedron Lett.* **39**, 537–540 (1998).
10. Creasy, L. L. & Coffee, M. Phytoalexin production potential of grape berries. *J. Am. Soc. Hortic. Sci.* **113**, 230–234 (1988).
11. Jeandet, P., Bessis, R. & Gautheron, B. The Production of Resveratrol (3,5,4'-trihydroxystilbene) by Grape Berries in Different Developmental Stages. *Am. J. Enol. Vitic.* **42**, 41–46 (1991).
12. Siemann, E. H. & Creasy, L. L. Concentration of the Phytoalexin Resveratrol in Wine. *Am. J. Enol. Vitic.* **43**, 49–52 (1992).
13. Nonomura, S., Kanagawa, H. & Makimoto, A. Chemical constituents of polygonaceous plants. I. Studies on the components of Ko-jo-kon (Polygonum cuspidatum Sieb Et Zucc.). *Yakugaku Zasshi* **83**, 988–990 (1963).
14. Renaud, S. & de Lorgeril, M. Wine, alcohol, platelets, and the French paradox for coronary heart disease. *Lancet* **339**, 1523–1526 (1992).
15. Jang, M. *et al.* Cancer chemopreventive activity of resveratrol, a natural product derived from grapes. *Science.* **275**, 218–220 (1997).
16. Pezzuto, J. M. The phenomenon of resveratrol: Redefining the virtues of promiscuity. *Ann. N. Y. Acad. Sci.* **1215**, 123–130 (2011).
17. Rivière, C., Pawlus, A. D. & Mérillon, J. M. Natural stilbenoids: Distribution in the plant kingdom and chemotaxonomic interest in Vitaceae. *Nat. Prod. Rep.* **29**, 1317–1333 (2012).
18. Shen, T., Wang, X. N. & Lou, H. X. Natural stilbenes: An overview. *Nat. Prod. Rep.* **26**, 916–935 (2009).
19. Keylor, M. H., Matsuura, B. S. & Stephenson, C. R. J. Chemistry and Biology of Resveratrol-Derived Natural Products. *Chem. Rev.* **115**, 8976–9027 (2015).
20. Cai, H. *et al.* Cancer chemoprevention: Evidence of a nonlinear dose response for the protective effects of resveratrol in humans and mice. *Sci. Transl. Med.* **7**, 298ra117- (2015).
21. de Sá Coutinho, D., Pacheco, M. T., Frozza, R. L. & Bernardi, A. Anti-inflammatory effects of resveratrol: Mechanistic insights. *Int. J. Mol. Sci.* **19**, 1812- (2018).
22. Rauf, A. *et al.* Resveratrol as an anti-cancer agent: A review. *Crit. Rev. Food Sci. Nutr.* **58**, 1428–1447 (2018).
23. Varoni, E. M., Lo Faro, A. F., Sharifi-Rad, J. & Iriti, M. Anticancer Molecular Mechanisms of Resveratrol. *Front. Nutr.* **3**, 8- (2016).

24. Zordoky, B. N. M., Robertson, I. M. & Dyck, J. R. B. Preclinical and clinical evidence for the role of resveratrol in the treatment of cardiovascular diseases. *Biochim. Biophys. Acta - Mol. Basis Dis.* **1852**, 1155–1177 (2014).
25. Prysyazhna, O. *et al.* Blood Pressure-Lowering by the Antioxidant Resveratrol Is Counterintuitively Mediated by Oxidation of cGMP-Dependent Protein Kinase. *Circulation* **140**, 126–137 (2019).
26. Bastianetto, S., Ménard, C. & Quirion, R. Neuroprotective action of resveratrol. *Biochim. Biophys. Acta - Mol. Basis Dis.* **1852**, 1195–1201 (2015).
27. Uddin, M. S. *et al.* Neuroprotective role of polyphenols against oxidative stress-mediated neurodegeneration. *Eur. J. Pharmacol.* **886**, 173412 (2020).
28. Uddin, M. S. *et al.* Natural products for neurodegeneration: regulating neurotrophic signals. *Oxid. Med. Cell. Longev.* **2021**, 8820406 (2021).
29. Gabaston, J. *et al.* Stilbenes from Vitis vinifera L. Waste: a sustainable tool for controlling Plasmopara viticola. *J. Agric. Food Chem.* **65**, 2711–2718 (2017).
30. Houillé, B. *et al.* Antifungal activity of resveratrol derivatives against Candida Species. *J. Nat. Prod.* **77**, 1658–1662 (2014).
31. Boo, Y. C. Human skin lightening efficacy of resveratrol and its analogs: From in vitro studies to cosmetic applications. *Antioxidants* **8**, 322 (2019).
32. Jeandet, P., Clément, C., Tisserant, L. P., Crouzet, J. & Courot, É. Use of grapevine cell cultures for the production of phytostilbenes of cosmetic interest. *Comptes Rendus Chim.* **19**, 1062–1070 (2016).
33. Kapetanovic, I. M., Muzzio, M., Huang, Z., Thompson, T. N. & McCormick, D. L. Pharmacokinetics, oral bioavailability, and metabolic profile of resveratrol and its dimethylether analog, pterostilbene, in rats. *Cancer Chemother. Pharmacol.* **68**, 593–601 (2011).
34. Walle, T. Bioavailability of resveratrol. *Ann. N. Y. Acad. Sci.* **1215**, 9–15 (2011).
35. Walle, T., Hsieh, F., DeLegge, M. H., Oatis, J. E. & Walle, U. K. High absorption but very low bioavailability of oral resveratrol in humans. *Drug Metab. Dispos.* **32**, 1377–1382 (2004).
36. Keylor, M. H. *et al.* Synthesis of resveratrol tetramers via a stereoconvergent radical equilibrium. *Science.* **354**, 1260–1265 (2016).
37. Snyder, S. A., Gollner, A. & Chiriac, M. I. Regioselective reactions for programmable resveratrol oligomer synthesis. *Nature* **474**, 461–466 (2011).
38. Donnez, D., Jeandet, P., Clément, C. & Courot, E. Bioproduction of resveratrol and stilbene derivatives by plant cells and microorganisms. *Trends Biotechnol.* **27**, 706–713 (2009).
39. Jeandet, P. *et al.* Whole-cell biocatalytic, enzymatic and green chemistry methods for the production of resveratrol and its derivatives. *Biotechnol. Adv.* **39**, 107461 (2020).
40. Martínez-Márquez, A. *et al.* Production of highly bioactive resveratrol analogues pterostilbene and piceatannol in metabolically engineered grapevine cell cultures. *Plant Biotechnol. J.* **14**, 1813–1825 (2016).
41. Ito, T. *et al.* Three new resveratrol oligomers from the stem bark of Vatica pauciflora. *J. Nat. Prod.* **67**, 932–937 (2004).
42. Nabavi, S. M. *et al.* Flavonoid biosynthetic pathways in plants: Versatile targets for metabolic engineering. *Biotechnol. Adv.* **38**, 107316 (2020).
43. Qian, Y. *et al.* Completion of the cytosolic post-chorismate phenylalanine biosynthetic pathway in plants. *Nat. Commun.* **10**, 47907 (2019).
44. Austin, M. B. & Noel, J. P. The chalcone synthase superfamily of type III polyketide synthases. *Nat. Prod. Rep.* **20**, 79–110 (2003).
45. Austin, M. B., Bowman, M. E., Ferrer, J. L., Schröder, J. & Noel, J. P. An aldol switch discovered in stilbene synthases mediates cyclization specificity of type III polyketide synthases. *Chem. Biol.* **11**, 1179–1194 (2004).
46. Smoliga, J. M. & Blanchard, O. Enhancing the delivery of resveratrol in humans: If low bioavailability is the problem, what is the solution? *Molecules* **19**, 17154–17172 (2014).

47. Caruso, F. *et al.* Antifungal activity of resveratrol against botrytis cinerea is improved using 2-furyl derivatives. *PLoS One* **6**, 25421 (2011).
48. Walle, T., Walle, U. K., Sedmera, D. & Klausner, M. Benzo[a]pyrene-induced oral carcinogenesis and chemoprevention: Studies in bioengineered human tissue. *Drug Metab. Dispos.* **34**, 346–350 (2006).
49. Goldberg, D. M., Yan, J. & Soleas, G. J. Absorption of three wine-related polyphenols in three different matrices by healthy subjects. *Clin. Biochem.* **36**, 79–87 (2003).
50. Springer, M. & Moco, S. Resveratrol and Its Human Metabolites—Effects on Metabolic Health and Obesity. *Nutrients* **11**, 143 (2019).
51. Böhmdorfer, M. *et al.* Involvement of UDP-glucuronosyltransferases and sulfotransferases in the excretion and tissue distribution of resveratrol in mice. *Nutrients* **9**, 1347 (2017).
52. Boocock, D. J. *et al.* Phase I dose escalation pharmacokinetic study in healthy volunteers of resveratrol, a potential cancer chemopreventive agent. *Cancer Epidemiol. Biomarkers Prev.* **16**, 1246–1252 (2007).
53. Miksits, M. *et al.* Sulfation of resveratrol in human liver: Evidence of a major role for the sulfotransferases SULT1A1 and SULT1E1. *Xenobiotica* **35**, 1101–1119 (2005).
54. Wu, B., Basu, S., Meng, S., Wang, X. & Hu, M. Regioselective Sulfation and Glucuronidation of Phenolics: Insights into the Structural Basis. *Curr. Drug Metab.* **12**, 900–916 (2012).
55. Lin, H. S., Yue, B. De & Ho, P. C. Determination of pterostilbene in rat plasma by a simple HPLC-UV method and its application in pre-clinical pharmacokinetic study. *Biomed. Chromatogr.* **23**, 1308–1315 (2009).
56. La Porte, C. *et al.* Steady-state pharmacokinetics and tolerability of trans-resveratrol 2000mg twice daily with food, quercetin and alcohol (Ethanol) in healthy human subjects. *Clin. Pharmacokinet.* **49**, 449–454 (2010).
57. Brown, V. A. *et al.* Repeat dose study of the cancer chemopreventive agent resveratrol in healthy volunteers: Safety, pharmacokinetics, and effect on the insulin-like growth factor axis. *Cancer Res.* **70**, 9003–9011 (2010).
58. Draijer, R. *et al.* Impact of proteins on the uptake, distribution, and excretion of phenolics in the human body. *Nutrients* **8**, 814 (2016).
59. Howells, L. M. *et al.* Phase I randomized, double-blind pilot study of micronized resveratrol (SRT501) in patients with hepatic metastases - Safety, pharmacokinetics, and pharmacodynamics. *Cancer Prev. Res.* **4**, 1419–1425 (2011).
60. Novotny, J. A. *et al.* The effect of obesity and repeated exposure on pharmacokinetic response to grape polyphenols in humans. *Mol. Nutr. Food Res.* **61**, 1700043 (2017).
61. Wightman, E. L. *et al.* The effects of chronic trans-resveratrol supplementation on aspects of cognitive function, mood, sleep, health and cerebral blood flow in healthy, young humans. *Br. J. Nutr.* **114**, 1427–1437 (2013).
62. Wong, R. H. X. *et al.* Acute resveratrol supplementation improves flow-mediated dilatation in overweight/obese individuals with mildly elevated blood pressure. *Nutr. Metab. Cardiovasc. Dis.* **21**, 851–856 (2011).
63. Bonnet, V., Gervaise, C., Djedaïni-Pilard, F., Furlan, A. & Sarazin, C. Cyclodextrin nanoassemblies: A promising tool for drug delivery. *Drug Discov. Today* **20**, 1120–1126 (2015).
64. Stella, V. J. & Rajewski, R. A. Sulfobutylether-β-cyclodextrin. *Int. J. Pharm.* **583**, 119396 (2020).
65. Din, F. U. *et al.* Effective use of nanocarriers as drug delivery systems for the treatment of selected tumors. *Int. J. Nanomedicine* **12**, 7291–7309 (2017).
66. Pinho, E., Grootveld, M., Soares, G. & Henriques, M. Cyclodextrins as encapsulation agents for plant bioactive compounds. *Carbohydr. Polym.* **101**, 121–135 (2014).
67. Gidwani, B. & Vyas, A. A Comprehensive Review on Cyclodextrin-Based Carriers for Delivery of Chemotherapeutic Cytotoxic Anticancer Drugs. *Biomed Res. Int.* **2015**, 198268 (2015).
68. Jones, S. T. *et al.* Modified cyclodextrins as broad-spectrum antivirals. *Sci. Adv.* **6**, eaax9318 (2020).
69. Argenziano, M. *et al.* Biological effect evaluation of glutathione-responsive cyclodextrin-based

nanosponges: 2D and 3D studies. *Molecules* **25**, 2775 (2020).
70. Gigliotti, C. L. *et al.* In vitro and in vivo therapeutic evaluation of camptothecin-encapsulated β-cyclodextrin nanosponges in prostate cancer. *J. Biomed. Nanotechnol.* **12**, 114–127 (2016).
71. A. Ansari, K., J. Torne, S., Pradeep R. Vavia, P., Trotta, F. & Cavalli, R. Paclitaxel Loaded Nanosponges: In-Vitro Characterization and Cytotoxicity Study on MCF-7 Cell Line Culture. *Curr. Drug Deliv.* **8**, 194–202 (2011).
72. Dora, C. P. *et al.* Potential of erlotinib cyclodextrin nanosponge complex to enhance solubility, dissolution rate, in vitro cytotoxicity and oral bioavailability. *Carbohydr. Polym.* **137**, 339–349 (2016).
73. Torne, S., Darandale, S., Vavia, P., Trotta, F. & Cavalli, R. Cyclodextrin-based nanosponges: effective nanocarrier for tamoxifen delivery. *Pharm. Dev. Technol.* **18**, 619–625 (2013).
74. Shende, P. K. *et al.* Influence of different techniques on formulation and comparative characterization of inclusion complexes of ASA with β-cyclodextrin and inclusion complexes of ASA with PMDA cross-linked β-cyclodextrin nanosponges. *J. Incl. Phenom. Macrocycl. Chem.* **74**, 447–454 (2012).
75. Mennini, N., Cirri, M., Maestrelli, F. & Mura, P. Comparison of liposomal and NLC (nanostructured lipid carrier) formulations for improving the transdermal delivery of oxaprozin: Effect of cyclodextrin complexation. *Int. J. Pharm.* **515**, 684–691 (2016).
76. Rao, M. R. P., Chaudhari, J., Trotta, F. & Caldera, F. Investigation of Cyclodextrin-Based Nanosponges for Solubility and Bioavailability Enhancement of Rilpivirine. *AAPS PharmSciTech* **19**, 2358–2369 (2018).
77. Adeoye, O. *et al.* Pyromellitic dianhydride crosslinked soluble cyclodextrin polymers: Synthesis, lopinavir release from sub-micron sized particles and anti-HIV-1 activity. *Int. J. Pharm.* **583**, 119356 (2020).
78. Sharma, R. & Pathak, K. Polymeric nanosponges as an alternative carrier for improved retention of econazole nitrate onto the skin through topical hydrogel formulation. *Pharm. Dev. Technol.* **16**, 367–376 (2011).
79. Mendes, C. *et al.* Cyclodextrin based nanosponge of norfloxacin: Intestinal permeation enhancement and improved antibacterial activity. *Carbohydr. Polym.* **195**, 586–592 (2018).
80. Trotta, F. *et al.* Molecularly imprinted cyclodextrin nanosponges for the controlled delivery of L-DOPA: perspectives for the treatment of Parkinson's disease. *Expert Opin. Drug Deliv.* **13**, 1671–1680 (2016).
81. Wong, K. H. *et al.* Delivering crocetin across the blood-brain barrier by using γ-cyclodextrin to treat Alzheimer's disease. *Sci. Rep.* **10**, 1–12 (2020).
82. Wong, K. H. *et al.* Review of current strategies for delivering Alzheimer's disease drugs across the blood-brain barrier. *Int. J. Mol. Sci.* **20**, 381 (2019).
83. Crini, G. Review: A history of cyclodextrins. *Chem. Rev.* **114**, 10940–10975 (2014).
84. Manor, P. C. & Saenger, W. Water molecule in hydrophobic surroundings: Structure of α-cyclodextrin-hexahydrate (C6H10O5) 6·6H2O. *Nature* **237**, 392–393 (1972).
85. Sandilya, A. A., Natarajan, U. & Priya, M. H. Molecular View into the Cyclodextrin Cavity: Structure and Hydration. *ACS Omega* **5**, 25655–25667 (2020).
86. Ikuta, D. *et al.* Conformationally supple glucose monomers enable synthesis of the smallest cyclodextrins. *Science.* **364**, 674–677 (2019).
87. Kanaya, A., Takashima, Y. & Harada, A. Double-threaded dimer and supramolecular oligomer formed by stilbene modified cyclodextrin: Effect of acyl migration and photostimuli. *J. Org. Chem.* **76**, 492–499 (2011).
88. Haley, R. M. *et al.* Resveratrol delivery from implanted cyclodextrin polymers provides sustained antioxidant effect on implanted neural probes. *Int. J. Mol. Sci.* **21**, 3579 (2020).
89. Connors, K. A. The stability of cyclodextrin complexes in solution. *Chem. Rev.* **97**, 1325–1357 (1997).
90. Sabadini, E., Cosgrove, T. & Egídio, F. D. C. Solubility of cyclomaltooligosaccharides (cyclodextrins) in H2O and D2O: A comparative study. *Carbohydr. Res.* **341**, 270–274 (2006).

91. Saenger, W. *et al.* Structures of the common cyclodextrins and their larger analogues - beyond the doughnut. *Chem. Rev.* **98**, 1787–1802 (1998).
92. Szejtli, J. Introduction and general overview of cyclodextrin chemistry. *Chem. Rev.* **98**, 1743–1753 (1998).
93. Lucas-Abellán, C., Fortea, I., López-Nicolás, J. M. & Núñez-Delicado, E. Cyclodextrins as resveratrol carrier system. *Food Chem.* **104**, 39–44 (2007).
94. Soo, E. *et al.* Enhancing delivery and cytotoxicity of resveratrol through a dual nanoencapsulation approach. *J. Colloid Interface Sci.* **462**, 368–374 (2016).
95. Tan, C., Wang, J. & Sun, B. Biopolymer-liposome hybrid systems for controlled delivery of bioactive compounds: Recent advances. *Biotechnol. Adv.* **48**, 107727 (2021).
96. Ciesielska, A. *et al.* Biomedical application of cyclodextrin polymers cross-linked via dianhydrides of carboxylic acids. *Appl. Sci.* **10**, 1–13 (2020).
97. Dhakar, N. K. *et al.* Comparative evaluation of solubility, cytotoxicity and photostability studies of resveratrol and oxyresveratrol loaded nanosponges. *Pharmaceutics* **11**, 545 (2019).
98. Yaşayan, G., Şatıroğlu Sert, B., Tatar, E. & Küçükgüzel, İ. Fabrication and characterisation studies of cyclodextrin-based nanosponges for sulfamethoxazole delivery. *J. Incl. Phenom. Macrocycl. Chem.* **97**, 175–186 (2020).
99. Palminteri, M. *et al.* Cyclodextrin nanosponge for the gsh-mediated delivery of resveratrol in human cancer cells. *Nanotheranostics* **5**, 197–212 (2021).
100. Ansari, K. A., Vavia, P. R., Trotta, F. & Cavalli, R. Cyclodextrin-based nanosponges for delivery of resveratrol: In vitro characterisation, stability, cytotoxicity and permeation study. *AAPS PharmSciTech* **12**, 279–286 (2011).
101. Tayo, L. L. Stimuli-responsive nanocarriers for intracellular delivery. *Biophys. Rev.* **9**, 931–940 (2017).
102. Babin, J. *et al.* A new two-photon-sensitive block copolymer nanocarrier. *Angew. Chemie - Int. Ed.* **48**, 3329–3332 (2009).
103. Wajs, E., Nielsen, T. T., Larsen, K. L. & Fragoso, A. Preparation of stimuli-responsive nano-sized capsules based on cyclodextrin polymers with redox or light switching properties. *Nano Res.* **9**, 2070–2078 (2016).
104. Wu, M. *et al.* Novel self-assembled pH-responsive biomimetic nanocarriers for drug delivery. *Mater. Sci. Eng. C* **64**, 346–353 (2016).
105. Manchun, S., Dass, C. R. & Sriamornsak, P. Targeted therapy for cancer using pH-responsive nanocarrier systems. *Life Sci.* **90**, 381–387 (2012).
106. Boedtkjer, E. & Pedersen, S. F. The Acidic Tumor Microenvironment as a Driver of Cancer. *Annu. Rev. Physiol.* **82**, 103–126 (2020).
107. Lin, J. T. *et al.* pH and redox dual stimulate-responsive nanocarriers based on hyaluronic acid coated mesoporous silica for targeted drug delivery. *Mater. Sci. Eng. C* **81**, 478–484 (2017).
108. Cheng, C. *et al.* Biotinylated thermoresponsive micelle self-assembled from double-hydrophilic block copolymer for drug delivery and tumor target. *Biomaterials* **29**, 497–505 (2008).
109. Kim, Y. J. & Matsunaga, Y. T. Thermo-responsive polymers and their application as smart biomaterials. *J. Mater. Chem. B* **5**, 4307–4321 (2017).
110. Kennedy, L., Sandhu, J. K., Harper, M. E. & Cuperlovic-culf, M. Role of glutathione in cancer: From mechanisms to therapies. *Biomolecules* **10**, 1–27 (2020).
111. Arunachalam, B., Phan, U. T., Geuze, H. J. & Cresswell, P. Enzymatic reduction of disulfide bonds in lysosomes: Characterization of a gamma-interferon-inducible lysosomal thiol reductase (GILT). *Proc. Natl. Acad. Sci. U. S. A.* **97**, 745–750 (2000).
112. Trotta, F. *et al.* Glutathione Bioresponsive Cyclodextrin Nanosponges. *Chempluschem* **81**, 439–443 (2016).
113. Daga, M. *et al.* GSH-targeted nanosponges increase doxorubicin-induced toxicity 'in vitro' and 'in vivo' in cancer cells with high antioxidant defenses. *Free Radic. Biol. Med.* **97**, 24–37 (2016).

114. Paczkowska, M. *et al.* Complex of rutin with β-cyclodextrin as potential delivery system. *PLoS One* **10**, e0120858 (2015).
115. Manta, K. *et al.* Preparation and Biophysical Characterization of Quercetin Inclusion Complexes with β-Cyclodextrin Derivatives to be Formulated as Possible Nose-to-Brain Quercetin Delivery Systems. *Mol. Pharm.* **17**, 4241–4255 (2020).
116. Gratieri, T. *et al.* Hydroxypropyl-β-cyclodextrin-complexed naringenin by solvent change precipitation for improving anti-inflammatory effect in vivo. *Carbohydr. Polym.* **231**, 115769 (2020).
117. Fumić, B., Jablan, J., Cinčić, D., Zovko Končić, M. & Jug, M. Cyclodextrin encapsulation of daidzein and genistein by grinding: implication on the glycosaminoglycan accumulation in mucopolysaccharidosis type II and III fibroblasts. *J. Microencapsul.* **35**, 1–12 (2018).
118. Rafati, N., Zarrabi, A., Caldera, F., Trotta, F. & Ghias, N. Pyromellitic dianhydride crosslinked cyclodextrin nanosponges for curcumin controlled release; formulation, physicochemical characterization and cytotoxicity investigations. *J. Microencapsul.* **36**, 715–727 (2019).
119. López-Nicolás, J. M., Rodríguez-Bonilla, P., Méndez-Cazorla, L. & García-Carmona, F. Physicochemical study of the complexation of pterostilbene by natural and modified cyclodextrins. *J. Agric. Food Chem.* **57**, 5294–5300 (2009).
120. Matencio, A., García-Carmona, F. & López-Nicolás, J. M. Encapsulation of piceatannol, a naturally occurring hydroxylated analogue of resveratrol, by natural and modified cyclodextrins. *Food Funct.* **7**, 2367–2373 (2016).
121. Silva, F., Figueiras, A., Gallardo, E., Nerín, C. & Domingues, F. C. Strategies to improve the solubility and stability of stilbene antioxidants: A comparative study between cyclodextrins and bile acids. *Food Chem.* **145**, 115–125 (2014).
122. Jambhekar, S. S. & Breen, P. Cyclodextrins in pharmaceutical formulations II: Solubilization, binding constant, and complexation efficiency. *Drug Discov. Today* **21**, 363–368 (2016).
123. Bertacche, V., Lorenzi, N., Nava, D., Pini, E. & Sinico, C. Host-guest interaction study of resveratrol with natural and modified cyclodextrins. *J. Incl. Phenom. Macrocycl. Chem.* **55**, 279–287 (2006).
124. Matencio, A., García-Carmona, F. & López-Nicolás, J. M. The inclusion complex of oxyresveratrol in modified cyclodextrins: A thermodynamic, structural, physicochemical, fluorescent and computational study. *Food Chem.* **232**, 177–184 (2017).
125. He, J. *et al.* Investigating the oxyresveratrol β-cyclodextrin and 2-hydroxypropyl-β-cyclodextrin complexes: The effects on oxyresveratrol solution, stability, and antibrowning ability on fresh grape juice. *LWT-Food Sci. Technol.* **100**, 263–270 (2019).
126. Stella, V. J., Rao, V. M., Zannou, E. A. & Zia, V. Mechanisms of drug release from cyclodextrin complexes. *Adv. Drug Deliv. Rev.* **36**, 3–16 (1999).
127. Venuti, V. *et al.* A characterization study of resveratrol/sulfobutyl ether-β-cyclodextrin inclusion complex and in vitro anticancer activity. *Colloids Surfaces B Biointerfaces* **115**, 22–28 (2014).
128. Kumpugdee-Vollrath, M., Ibold, Y. & Sriamornsak, P. Solid state characterization of trans resveratrol complexes with different cyclodextrins. *JAASP* **1**, 125–136 (2012).
129. Lopez-Nicolas, J. M., Rodríguez-Bonilla, P. & García-Carmona, F. Complexation of pinosylvin, an analogue of resveratrol with high antifungal and antimicrobial activity, by different types of cyclodextrins. *J. Agric. Food Chem.* **57**, 10175–10180 (2009).
130. Li, S. *et al.* Photostability and antioxidant activity studies on the inclusion complexes of: Trans -polydatin with β-cyclodextrin and derivatives. *RSC Adv.* **8**, 25941–25948 (2018).
131. Lu, Z., Cheng, B., Hu, Y., Zhang, Y. & Zou, G. Complexation of resveratrol with cyclodextrins: Solubility and antioxidant activity. *Food Chem.* **113**, 17–20 (2009).
132. Soussi, D. *et al.* Vectisol formulation enhances solubility of resveratrol and brings its benefits to kidney transplantation in a preclinical porcine model. *Int. J. Mol. Sci.* **20**, (2019).
133. Kong, D. *et al.* Pulmonary administration of resveratrol/hydroxypropyl-β-cyclodextrin inclusion complex: in vivo disposition and in vitro metabolic study. *J. Drug Deliv. Sci. Technol.*

60, 101995 (2020).
134. Sapino, S., Carlotti, M. E., Caron, G., Ugazio, E. & Cavalli, R. In silico design, photostability and biological properties of the complex resveratrol/hydroxypropyl-β-cyclodextrin. *J. Incl. Phenom. Macrocycl. Chem.* **63**, 171–180 (2009).
135. Silva, A. F. R. *et al.* Inclusion complex of resveratrol with γ-cyclodextrin as a functional ingredient for lemon juices. *Foods* **10**, 16 (2021).
136. Lim, Y. R. I. *et al.* Pterostilbene complexed with cyclodextrin exerts antimicrobial and anti-inflammatory effects. *Sci. Rep.* **10**, 1–10 (2020).
137. Berta, G. N. *et al.* Chemoprevention of 7,12-dimethylbenz[a]anthracene (DMBA)-induced oral carcinogenesis in hamster cheek pouch by topical application of resveratrol complexed with 2-hydroxypropyl-β-cyclodextrin. *Oral Oncol.* **46**, 42–48 (2010).
138. Lucas-Abellán, C., Fortea, M. I., Gabaldón, J. A. & Núñez-Delicado, E. Complexation of resveratrol by native and modified cyclodextrins: Determination of complexation constant by enzymatic, solubility and fluorimetric assays. *Food Chem.* **111**, 262–267 (2008).
139. Trollope, L. *et al.* Inclusion of trans-resveratrol in methylated cyclodextrins: Synthesis and solid-state structures. *Beilstein J. Org. Chem.* **10**, 3136–3151 (2014).
140. Duarte, A. *et al.* Resveratrol encapsulation with methyl-β-cyclodextrin for antibacterial and antioxidant delivery applications. *LWT-Food Sci. Technol.* **63**, 1254–1260 (2015).
141. Matencio, A. *et al.* Study of oxyresveratrol complexes with insoluble cyclodextrin based nanosponges: Developing a novel way to obtain their complexation constants and application in an anticancer study. *Carbohydr. Polym.* **231**, 115763 (2020).
142. Pushpalatha, R., Selvamuthukumar, S. & Kilimozhi, D. Carbonyl and carboxylate crosslinked cyclodextrin as a nanocarrier for resveratrol: in silico, in vitro and in vivo evaluation. *J. Incl. Phenom. Macrocycl. Chem.* **92**, 261–272 (2018).
143. Lu, Z., Chen, R., Fu, R., Xiong, J. & Hu, Y. Cytotoxicity and inhibition of lipid peroxidation activity of resveratrol/cyclodextrin inclusion complexes. *J. Incl. Phenom. Macrocycl. Chem.* **73**, 313–320 (2012).
144. Wang, X. *et al.* Inhalable resveratrol-cyclodextrin complex loaded biodegradable nanoparticles for enhanced efficacy against non-small cell lung cancer. *Int. J. Biol. Macromol.* **164**, 638–650 (2020).
145. Das, S., Lin, H. S., Ho, P. C. & Ng, K. Y. The impact of aqueous solubility and dose on the pharmacokinetic profiles of resveratrol. *Pharm. Res.* **25**, 2593–2600 (2008).
146. dos Santos Lima, B., Shanmugam, S., de Souza Siqueira Quintans, J., Quintans-Júnior, L. J. & de Souza Araújo, A. A. Inclusion complex with cyclodextrins enhances the bioavailability of flavonoid compounds: a systematic review. *Phytochem. Rev.* **18**, 1337–1359 (2019).
147. Allan, K. E., Lenehan, C. E. & Ellis, A. V. UV Light Stability of α-Cyclodextrin/Resveratrol Host-Guest Complexes and Isomer Stability at Varying pH. *Aust. J. Chem.* **62**, 921–926 (2009).
148. Gui Cheng, J., Ren Tian, B., Huang, Q., Rong Ge, H. & Zhong Wang, Z. Resveratrol Functionalized Carboxymethyl-β-Cyclodextrin: Synthesis, Characterization, and Photostability. *J. Chem.* **2018**, 6789076 (2018).
149. Bayomi, M. A., Abanumay, K. A. & Al-Angary, A. A. Effect of inclusion complexation with cyclodextrins on photostability of nifedipine in solid state. *Int. J. Pharm.* **243**, 107–117 (2002).
150. Trela, B. C. & Waterhouse, A. L. Resveratrol: Isomeric molar absorptivities and stability. *J. Agric. Food Chem.* **44**, 1253–1257 (1996).
151. dos Santos Lacerda, D. *et al.* Pterostilbene reduces oxidative stress, prevents hypertrophy and preserves systolic function of right ventricle in cor pulmonale model. *Br. J. Pharmacol.* **174**, 3302–3314 (2017).
152. Lacerda, D. *et al.* Stilbenoid pterostilbene complexed with cyclodextrin preserves left ventricular function after myocardial infarction in rats: possible involvement of thiol proteins and modulation of phosphorylated GSK-3β. *Free Radic. Res.* **52**, 988–999 (2018).
153. Vestergaardm, M. & Ingmer, H. Antibacterial and antifungal properties of resveratrol. *Int. J. Antimicrob. Agents* **53**, 716–723 (2019).

154. Costa, A., Bonner, M. Y. & Arbiser, J. L. Use of Polyphenolic Compounds in Dermatologic Oncology. *Am. J. Clin. Dermatol.* **17**, 369–385 (2016).
155. Lin, M.-H. *et al.* The Bioactivities of Resveratrol and Its Naturally Occurring Derivatives on Skin. *J. Food Drug Anal.* **29**, 15–38 (2021).
156. Aziz, M., Afaq, F. & Ahmad, N. Prevention of ultraviolet B radiation - damage by resveratrol in mouse skin is mediated via modulation in Survivin. *Photochem. Photobiol.* **81**, (2004).
157. Osmond, G. W., Augustine, C. K., Zipfel, P. A., Padussis, J. & Tyler, D. S. Enhancing melanoma treatment with resveratrol. *J. Surg. Res.* **172**, 109–115 (2012).
158. Sirerol, J. A. *et al.* Topical treatment with pterostilbene, a natural phytoalexin, effectively protects hairless mice against UVB radiation-induced skin damage and carcinogenesis. *Free Radic. Biol. Med.* **85**, 1–11 (2015).
159. Docherty, J. J., Smith, J. S., Fu, M. M., Stoner, T. & Booth, T. Effect of topically applied resveratrol on cutaneous herpes simplex virus infections in hairless mice. *Antiviral Res.* **61**, 19–26 (2004).
160. Kjær, T. N., Thorsen, K., Jessen, N., Stenderup, K. & Pedersen, S. B. Resveratrol ameliorates imiquimod-induced psoriasis-like skin inflammation in mice. *PLoS One* **10**, e0126599 (2015).
161. Pushpalatha, R., Selvamuthukumar, S. & Kilimozhi, D. Cyclodextrin nanosponge based hydrogel for the transdermal co-delivery of curcumin and resveratrol: Development, optimization, in vitro and ex vivo evaluation. *J. Drug Deliv. Sci. Technol.* **52**, 55–64 (2019).
162. Regev-Shoshani, G., Shoseyov, O., Bilkis, I. & Kerem, Z. Glycosylation of resveratrol protects it from enzymic oxidation. *Biochem. J.* **374**, 157–163 (2003).
163. González-Alfonso, J. L. *et al.* Enzymatic synthesis of a novel pterostilbene α-glucoside by the combination of cyclodextrin glucanotransferase and amyloglucosidase. *Molecules* **23**, 1271 (2018).
164. Marié, T. *et al.* Enzymatic synthesis of resveratrol α-glycosides from β-cyclodextrin-resveratrol complex in water. *ACS Sustain. Chem. Eng.* **6**, 5370–5380 (2018).
165. Ioannou, I. *et al.* Implementation of an enzyme membrane reactor to intensify the α-O-glycosylation of resveratrol using cyclodextrins. *Pharmaceuticals* **14**, 319 (2021).
166. Shimoda, K., Kubota, N., Hamada, H. & Hamada, H. Synthesis of resveratrol glycosides by plant glucosyltransferase and cyclodextrin glucanotransferase and their neuroprotective activity. *Nat. Prod. Commun.* **10**, 995–996 (2015).
167. De Winter, K. *et al.* Ionic liquids as cosolvents for glycosylation by sucrose phosphorylase: Balancing acceptor solubility and enzyme stability. *Green Chem.* **15**, 1949–1955 (2013).
168. Mathew, S., Hedström, M. & Adlercreutz, P. Enzymatic synthesis of piceid glycosides by cyclodextrin glucanotransferase. *Process Biochem.* **47**, 528–532 (2012).
169. Torres, P. *et al.* Enzymatic synthesis of α-glucosides of resveratrol with surfactant activity. *Adv. Synth. Catal.* **353**, 1077–1086 (2011).
170. Aramsangtienchai, P., Chavasiri, W., Ito, K. & Pongsawasdi, P. Synthesis of epicatechin glucosides by a β-cyclodextrin glycosyltransferase. *J. Mol. Catal. B Enzym.* **73**, 27–34 (2011).
171. Choung, W. J. *et al.* Enzymatic synthesis of a novel kaempferol-3-O-β- d -glucopyranosyl-(1→4)-O-α- d -glucopyranoside using cyclodextrin glucanotransferase and its inhibitory effects on aldose reductase, inflammation, and oxidative stress. *J. Agric. Food Chem.* **65**, 2760–2767 (2017).
172. Han, R. *et al.* High production of genistein diglucoside derivative using cyclodextrin glycosyltransferase from Paenibacillus macerans. *J. Ind. Microbiol. Biotechnol.* **44**, 1343–1354 (2017).
173. Lee, Y. S. *et al.* Glucosylation of flavonol and flavanones by Bacillus cyclodextrin glucosyltransferase to enhance their solubility and stability. *Food Chem.* **229**, 75–83 (2017).
174. Khummanee, N., Rudeekulthamrong, P. & Kaulpiboon, J. Cyclodextrin Glycosyltransferase-Catalyzed Synthesis of Pinoresinol-α-D-glucoside Having Antioxidant and Anti-Inflammatory Activities. *Appl. Biochem. Microbiol.* **55**, 360–370 (2019).
175. Mathew, S. & Adlercreutz, P. Regioselective glycosylation of hydroquinone to α-arbutin by

cyclodextrin glucanotransferase from Thermoanaerobacter sp. *Biochem. Eng. J.* **79**, 187–193 (2013).
176. Lim, C. H., Rasti, B., Sulistyo, J. & Hamid, M. A. Comprehensive study on transglycosylation of CGTase from various sources. *Heliyon* **7**, e06305 (2021).
177. Intagliata, S., Modica, M. N., Santagati, L. M. & Montenegro, L. Strategies to improve resveratrol systemic and topical bioavailability: An update. *Antioxidants* **8**, 244 (2019).
178. Rühlmann, A., Antovic, D., Müller, T. J. J. & Urlacher, V. B. Regioselective Hydroxylation of Stilbenes by Engineered Cytochrome P450 from Thermobifida fusca YX. *Adv. Synth. Catal.* **359**, 984–994 (2017).
179. Morales, M., Bru, R., García-Carmona, F., Ros Barceló, A. & Pedreño, M. A. Effect of dimethyl-β-cyclodextrins on resveratrol metabolism in Gamay grapevine cell cultures before and after inoculation with Xylophilus ampelinus. *Plant Cell. Tissue Organ Cult.* **53**, 179–187 (1998).
180. Bru, M. R. & Pedreno, M. A. Method for the production of resveratrol in cell cultures. (2003).
181. Bru, R., Sellés, S., Casado-Vela, J., Belchí-Navarro, S. & Pedreño, M. A. Modified cyclodextrins are chemically defined glucan inducers of defense responses in grapevine cell cultures. *J. Agric. Food Chem.* **54**, 66–71 (2006).
182. Zamboni, A. *et al.* Elicitor-induced resveratrol production in cell cultures of different grape genotypes (Vitis spp.). *Vitis* **45**, 63–68 (2006).
183. Ferri, M., Dipalo, S. C. F., Bagni, N. & Tassoni, A. Chitosan elicits mono-glucosylated stilbene production and release in fed-batch bioreactor cultures of grape cells. *Food Chem.* **124**, 1473–1479 (2011).
184. Nivelle, L. *et al.* Anti-cancer activity of resveratrol and derivatives produced by grapevine cell suspensions in a 14 L stirred bioreactor. *Molecules* **22**, 474 (2017).
185. Krisa, S. *et al.* Stilbene production by Vitis vinifera cell suspension cultures: Methyl jasmonate induction and 13C biolabeling. *J. Nat. Prod.* **62**, 1688–1690 (1999).
186. Tassoni, A. *et al.* Jasmonates and Na-orthovanadate promote resveratrol production in Vitis vinifera cv. Barbera cell cultures. *New Phytol.* **166**, 895–905 (2005).
187. Santamaria, A. R. *et al.* Stilbene production in cell cultures of Vitis vinifera L. cvs Red Globe and Michele Palieri elicited by methyl jasmonate. *Nat. Prod. Res.* **24**, 1488–1498 (2010).
188. Almagro, L., Belchí-Navarro, S., Martínez-Márquez, A., Bru, R. & Pedreño, M. A. Enhanced extracellular production of trans-resveratrol in Vitis vinifera suspension cultured cells by using cyclodextrins and coronatine. *Plant Physiol. Biochem.* **97**, 361–367 (2015).
189. Belchí-Navarro, S., Almagro, L., Lijavetzky, D., Bru, R. & Pedreño, M. A. Enhanced extracellular production of trans-resveratrol in Vitis vinifera suspension cultured cells by using cyclodextrins and methyljasmonate. *Plant Cell Rep.* **31**, 81–89 (2012).
190. Lijavetzky, D. *et al.* Synergistic effect of methyljasmonate and cyclodextrin on stilbene biosynthesis pathway gene expression and resveratrol production in Monastrell grapevine cell cultures. *BMC Res. Notes* **1**, 132 (2008).
191. Oliva, E. *et al.* Physico-chemical studies of resveratrol, methyl-jasmonate and cyclodextrin interactions: An approach to resveratrol bioproduction optimization. *RSC Adv.* **8**, 1528–1538 (2018).
192. Almagro, L. *et al.* A smart strategy to improve t-resveratrol production in grapevine cells treated with cyclodextrin polymers coated with magnetic nanoparticles. *Polymers (Basel).* **12**, 991 (2020).
193. Medina-Bolivar, F. *et al.* Production and secretion of resveratrol in hairy root cultures of peanut. *Phytochemistry* **68**, 1992–2003 (2007).
194. Nopo-Olazabal, C., Hubstenberger, J., Nopo-Olazabal, L. & Medina-Bolivar, F. Antioxidant activity of selected stilbenoids and their bioproduction in hairy root cultures of muscadine grape (vitis rotundifolia michx.). *J. Agric. Food Chem.* **61**, 11744–11758 (2013).
195. Tisserant, L. P. *et al.* Enhanced stilbene production and excretion in Vitis vinifera cv pinot noir hairy root cultures. *Molecules* **21**, 1703 (2016).
196. Yang, T. *et al.* Enhanced production of resveratrol, piceatannol, arachidin-1, and arachidin-3 in

hairy root cultures of peanut co-treated with methyl jasmonate and cyclodextrin. *J. Agric. Food Chem.* **63**, 3942–3950 (2015).
197. Fang, L., Yang, T. & Medina-Bolivar, F. Production of prenylated stilbenoids in hairy root cultures of peanut (Arachis hypogaea) and its wild relatives A. Ipaensis and A. duranensis via an optimized elicitation procedure. *Molecules* **25**, 509 (2020).
198. Jeandet, P., Clément, C. & Courot, E. Resveratrol production at large scale using plant cell suspensions. *Eng. Life Sci.* **14**, 622–632 (2014).
199. Aumont, V. *et al.* Production of highly 13C-labeled polyphenols in Vitis vinifera cell bioreactor cultures. *J. Biotechnol.* **109**, 287–294 (2004).
200. Lambert, C. *et al.* Optimize, modulate, and scale-up resveratrol and resveratrol dimers bioproduction in vitis labrusca l. Cell suspension from flasks to 20 l bioreactor. *Plants* **8**, 567 (2019).
201. Vera-Urbina, J. C., Selles-Marchart, S., Martinez-Esteso, M. J., Pedreño, M. A. & Bru-Martinez, R. Resveratrol: Sources, Production and Health Benefits. in (ed. Delmas, D.) 19–39 (Nova Science Publishers Inc, 2013).
202. Donnez, D. *et al.* Bioproduction of resveratrol and viniferins by an elicited grapevine cell culture in a 2 L stirred bioreactor. *Process Biochem.* **46**, 1056–1062 (2011).
203. Eibl, R. & Eibl, D. Design of bioreactors suitable for plant cell and tissue cultures. *Phytochem. Rev.* **7**, 593–598 (2007).
204. Martínez-Márquez, A., Morante-Carriel, J. A., Palazon, J. & Bru-Martínez, R. Rosa hybrida orcinol O-methyl transferase-mediated production of pterostilbene in metabolically engineered grapevine cell cultures. *N. Biotechnol.* **42**, 62–70 (2018).
205. Hidalgo, D. *et al.* Silybum marianum cell cultures stably transformed with Vitis vinifera stilbene synthase accumulate t-resveratrol in the extracellular medium after elicitation with methyl jasmonate or methylated β-cyclodextrins. *Eng. Life Sci.* **17**, 686–694 (2017).
206. Cervone, F., Hahn, M. G., de Lorenzo, G., Darvill, A. & Albersheim, P. Host-pathogen interactions: XXXIII. A plant protein converts a fungal pathogenesis factor into an elicitor of plant defense responses. *Plant Physiol.* **90**, 542–548 (1989).
207. Belchí-Navarro, S. *et al.* Early signaling events in grapevine cells elicited with cyclodextrins and methyl jasmonate. *Plant Physiol. Biochem.* **62**, 107–110 (2013).
208. Poinssot, B. *et al.* The endopolygalacturonase 1 from Botrytis cinerea activates grapevine defense reactions unrelated to its enzymatic activity. *Mol. Plant-Microbe Interact.* **16**, 553–564 (2003).
209. Vandelle, E., Poinssot, B., Wendehenne, D., Bentéjac, M. & Pugin, A. Integrated signaling network involving calcium, nitric oxide, and active oxygen species but not mitogen-activated protein kinases in BcPG1-elicited grapevine defenses. *IS-MPMI* **19**, 429–440 (2006).
210. Jiang, J. *et al.* VvWRKY8 represses stilbene synthase genes through direct interaction with VvMYB14 to control resveratrol biosynthesis in grapevine. *J. Exp. Bot.* **70**, 715–729 (2019).
211. Jeandet, P., Clément, C. & Cordelier, S. Regulation of resveratrol biosynthesis in grapevine: New approaches for disease resistance? *J. Exp. Bot.* **70**, 375–378 (2019).
212. Duan, D. *et al.* An ancestral allele of grapevine transcription factor MYB14 promotes plant defence. *J. Exp. Bot.* **67**, 1795–1804 (2016).
213. Wong, D. C. J. & Matus, J. T. Constructing integrated networks for identifying new secondary metabolic pathway regulators in grapevine: Recent applications and future opportunities. *Front. Plant Sci.* **8**, 505 (2017).
214. Vannozzi, A. *et al.* Combinatorial Regulation of Stilbene Synthase Genes by WRKY and MYB Transcription Factors in Grapevine (Vitis vinifera L.). *Plant Cell Physiol.* **59**, 1043–1059 (2018).
215. Höll, J. *et al.* The R2R3-MYB transcription factors MYB14 and MYB15 regulate stilbene biosynthesis in Vitis vinifera. *Plant Cell* **25**, 4135–4149 (2013).
216. Mitsuda, N. *et al.* NAC transcription factors, NST1 and NST3, are key regulators of the formation of secondary walls in woody tissues of Arabidopsis. *Plant Cell* **19**, 270–280 (2007).
217. Almagro, L. *et al.* Dissecting the transcriptional response to elicitors in Vitis vinifera cells. *PLoS*

One **9**, 109777 (2014).
218. Martínez-Márquez, A. *et al.* A tau class glutathione-S-transferase is involved in trans-resveratrol transport out of grapevine cells. *Front. Plant Sci.* **8**, 1457 (2017).
219. Martinez-Esteso, M. J., Sellés-Marchart, S., Vera-Urbina, J. C., Pedreño, M. A. & Bru-Martinez, R. DIGE analysis of proteome changes accompanying large resveratrol production by grapevine (Vitis vinifera cv. Gamay) cell cultures in response to methyl-β-cyclodextrin and methyl jasmonate elicitors. *J. Proteomics* **74**, 1421–1436 (2011).
220. Yang, T. *et al.* Stilbenoid prenyltransferases define key steps in the diversification of peanut phytoalexins. *J. Biol. Chem.* **293**, 28–46 (2018).

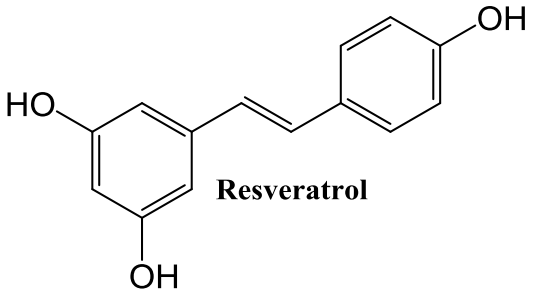

Resveratrol

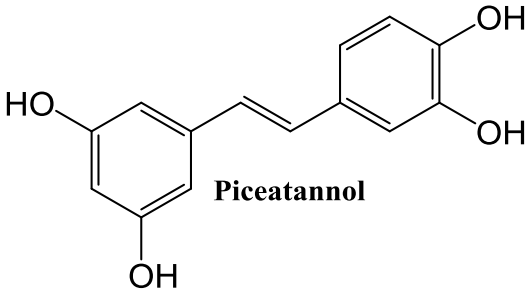

Piceatannol

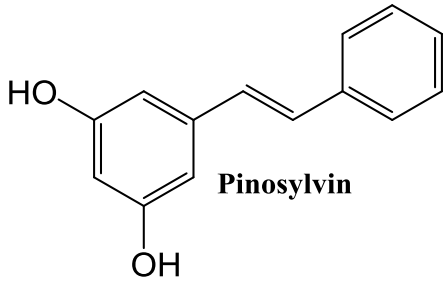

Pinosylvin

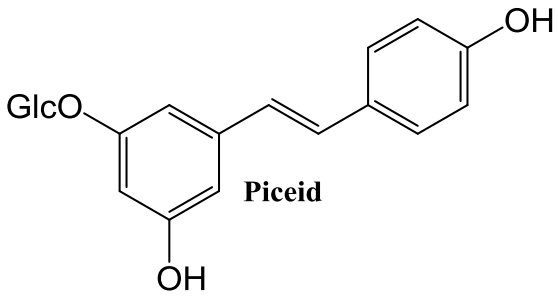

Piceid

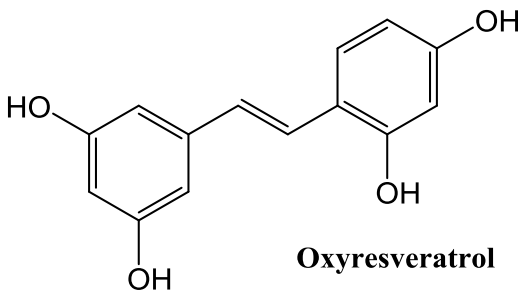

Oxyresveratrol

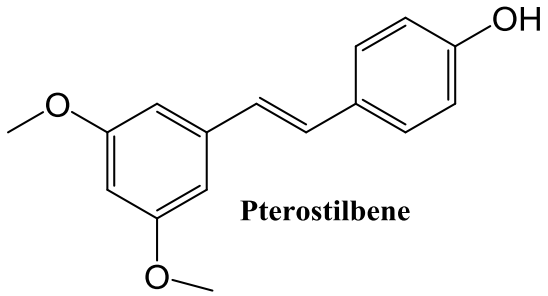

Pterostilbene

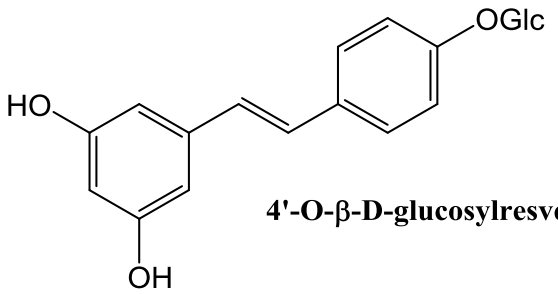

4'-O-β-D-glucosylresveratrol

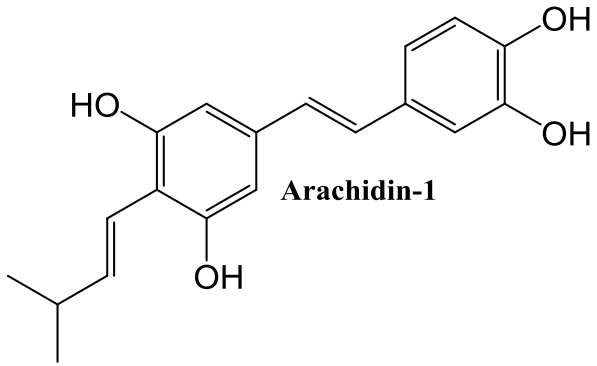

Arachidin-1

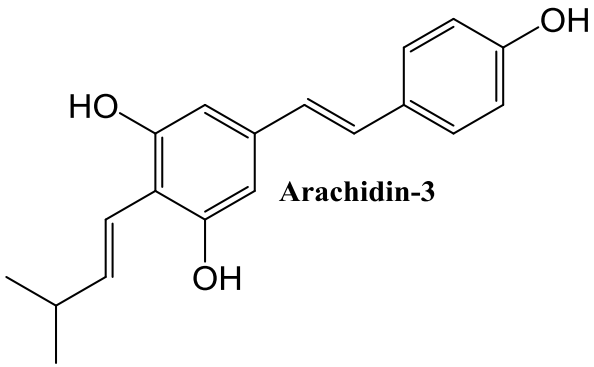

Arachidin-3

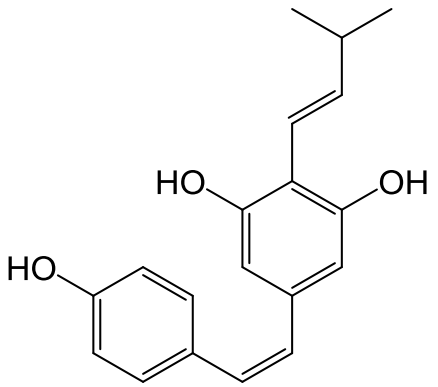

Arachidin-2

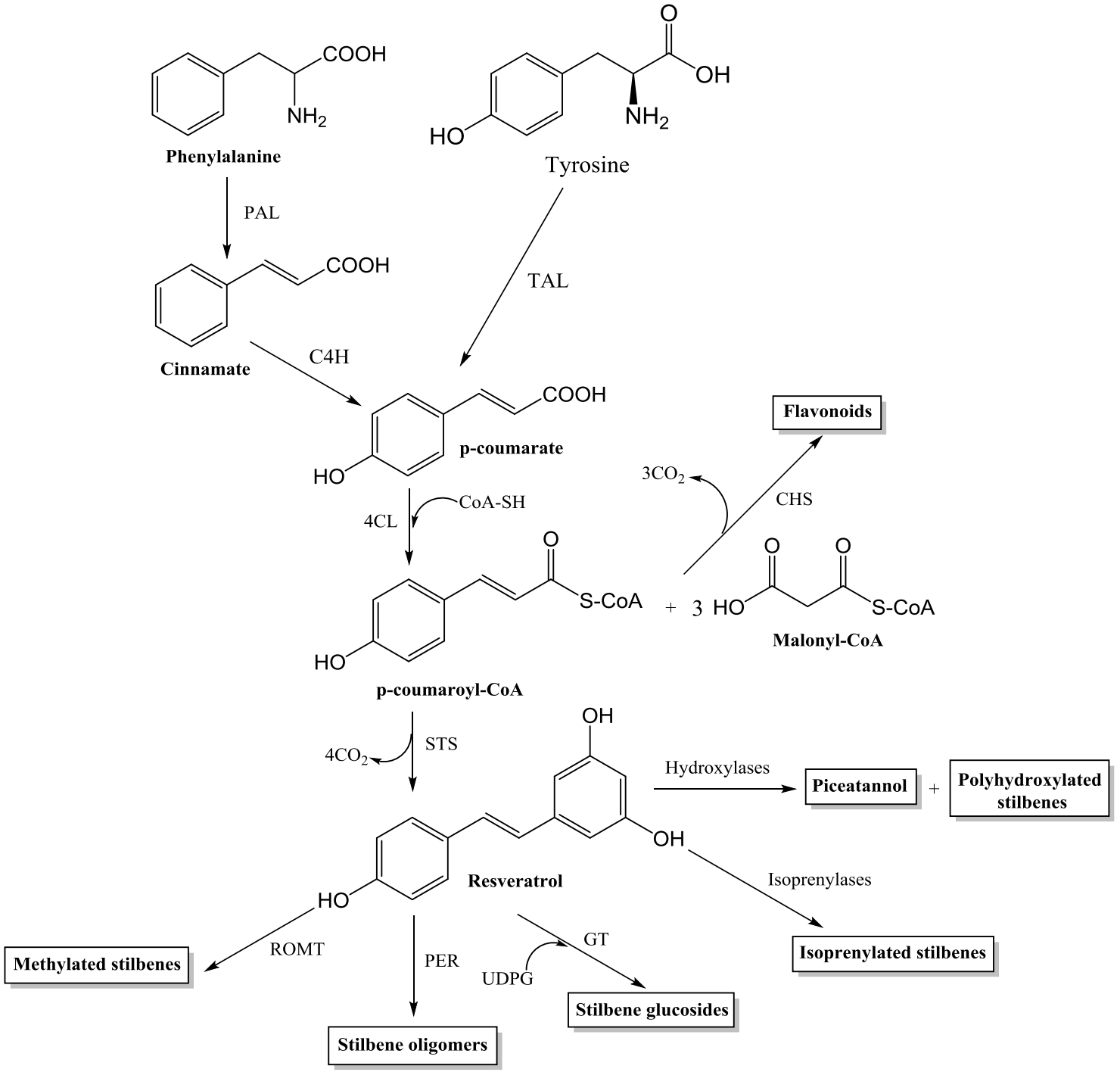
Phenylalanine
Tyrosine
PAL
TAL
Cinnamate
C4H
p-coumarate
4CL
CoA-SH
p-coumaroyl-CoA
3CO2
CHS
Flavonoids
+ 3
Malonyl-CoA
4CO2
STS
Resveratrol
Hydroxylases
Piceatannol
+
Polyhydroxylated stilbenes
Isoprenylases
Isoprenylated stilbenes
ROMT
Methylated stilbenes
PER
Stilbene oligomers
UDPG
GT
Stilbene glucosides

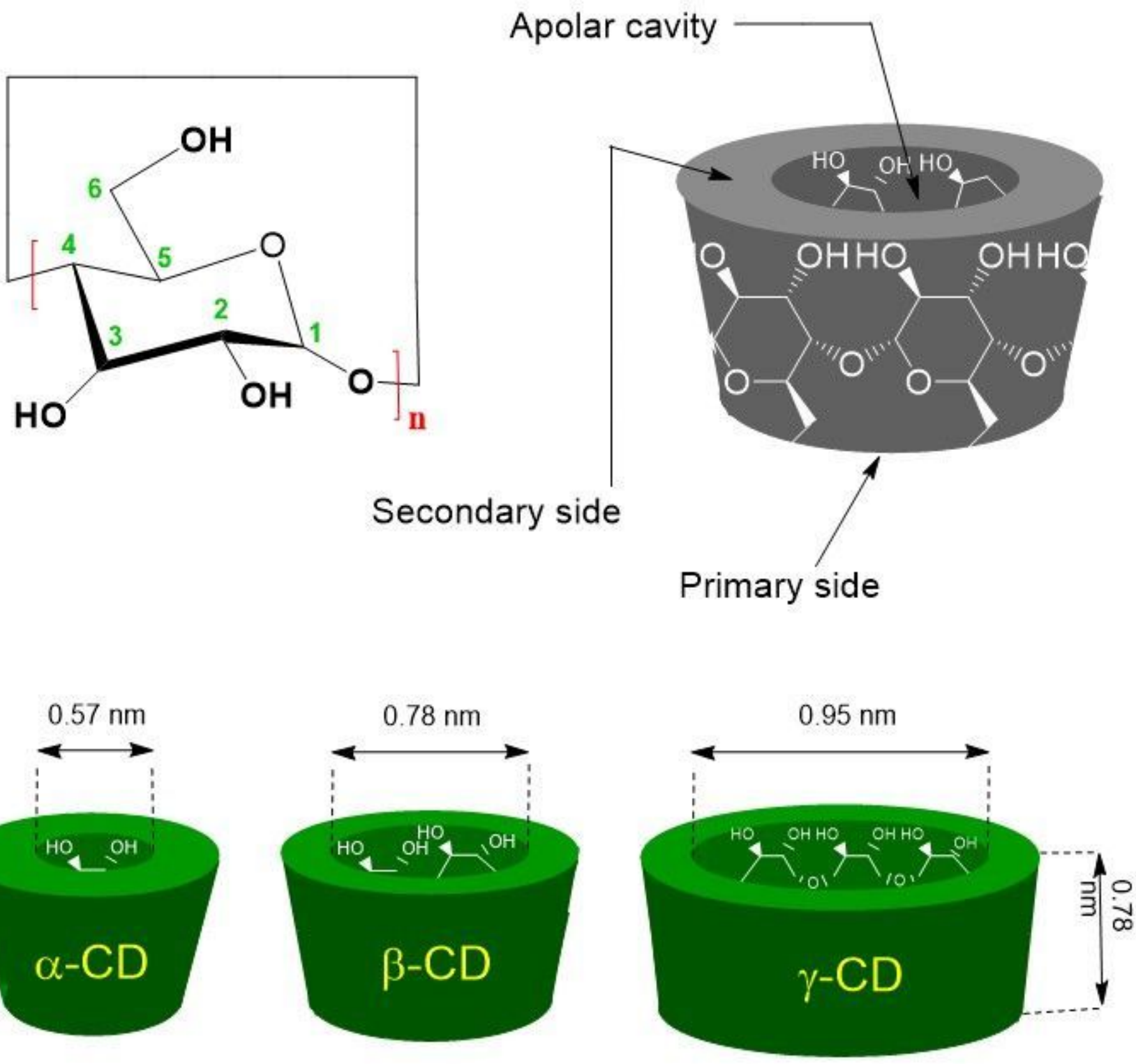
Apolar cavity
OH
6
4
5
O
3
2
1
HO
OH
O
n
HO
OH HO
OH HO
OH HO
Secondary side
Primary side
0.57 nm
0.78 nm
0.95 nm
HO
OH
α-CD
β-CD
γ-CD
0.78 nm

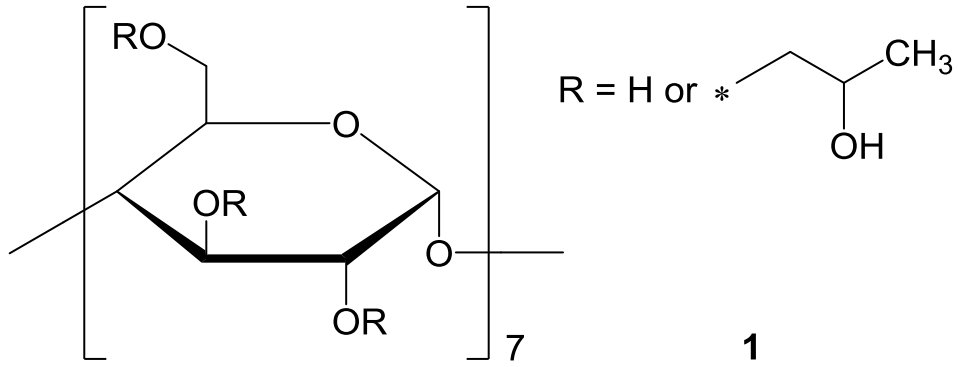
RO
O
OR
O
OR
7
R = H or *
CH3
OH

1

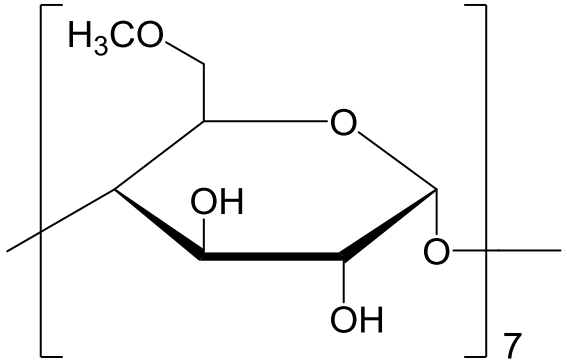
H3CO
O
OH
O
OH
7

2

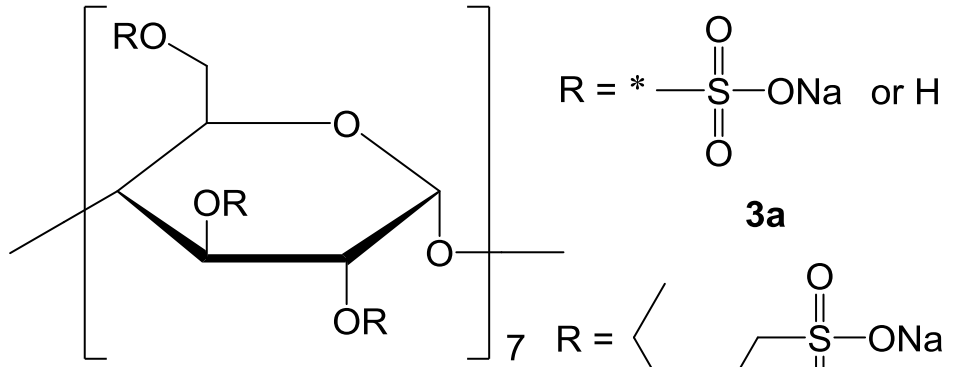
RO
O
OR
O
OR
7
R = *
S
ONa
or H
O
O
R =
S
ONa
O
O

3a

3b

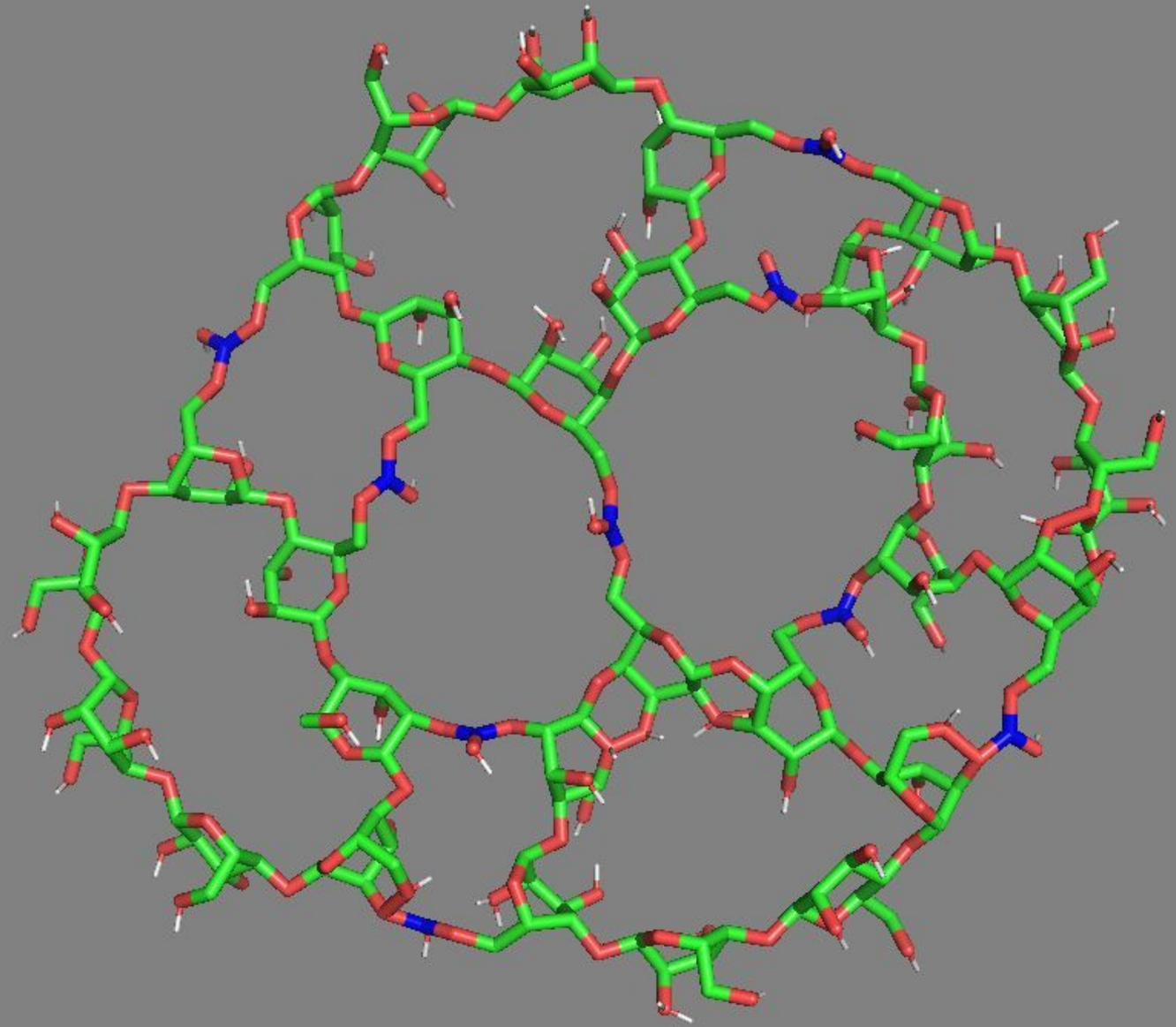

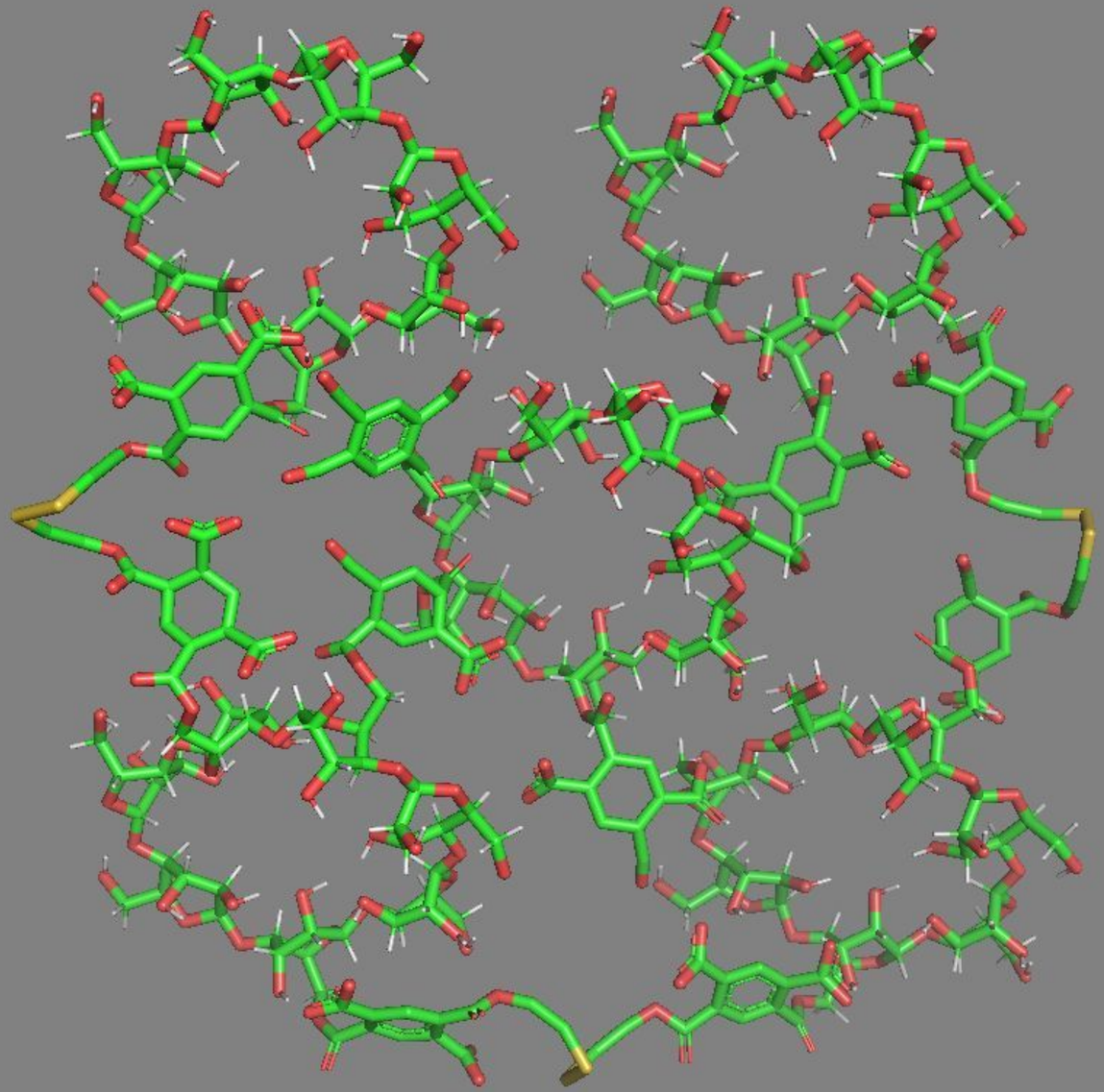

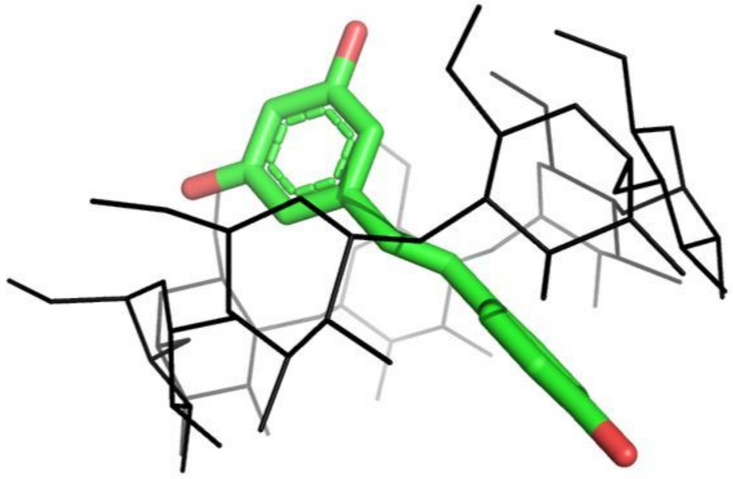
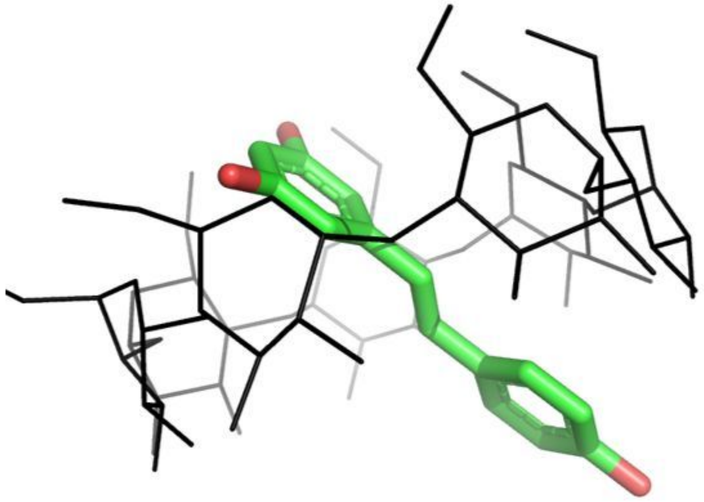
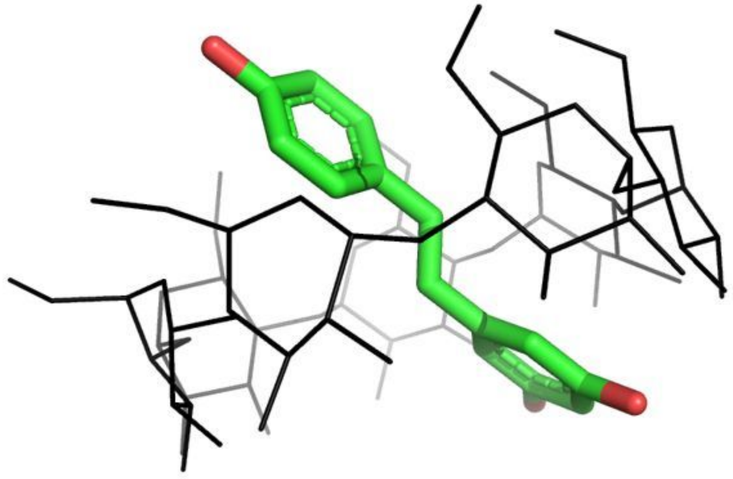
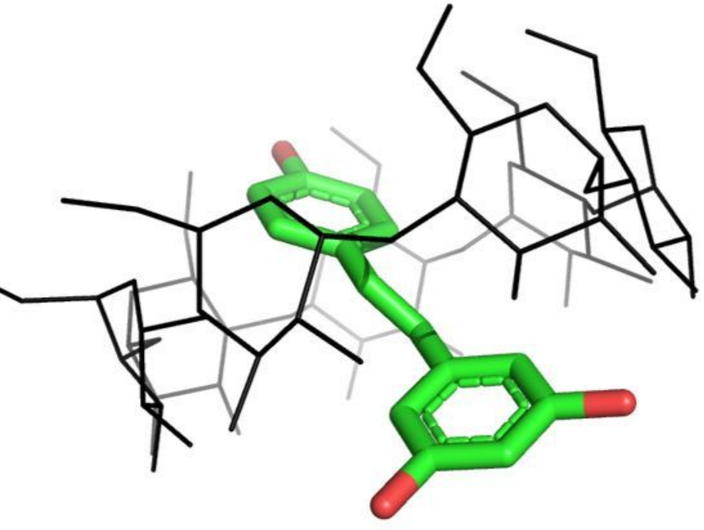
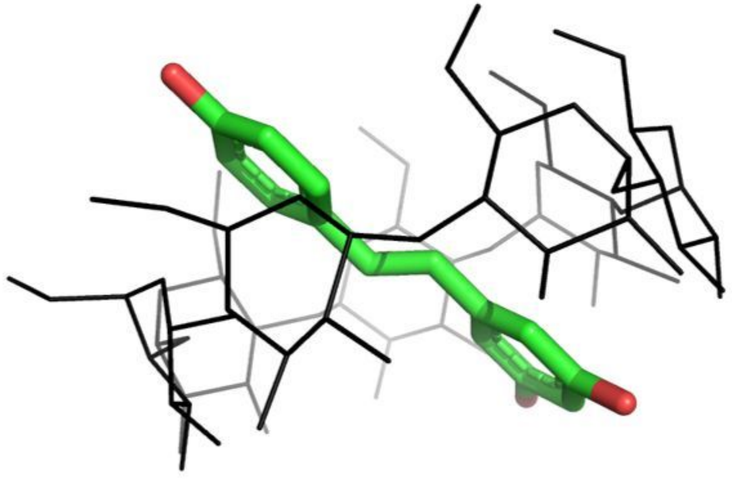
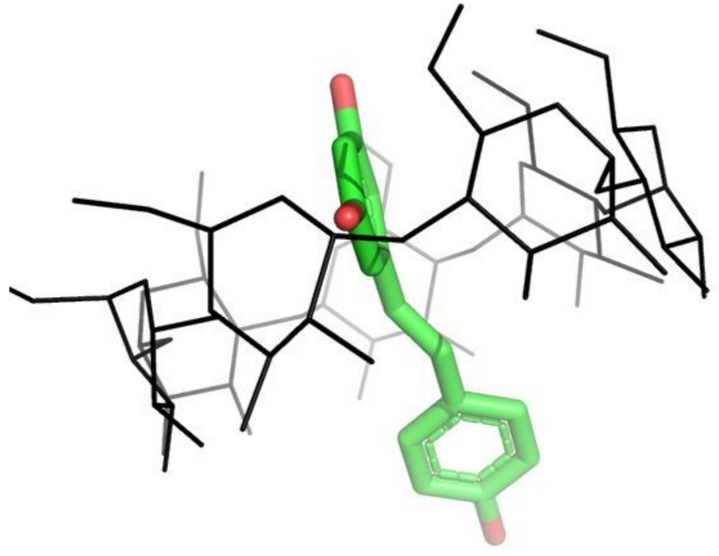

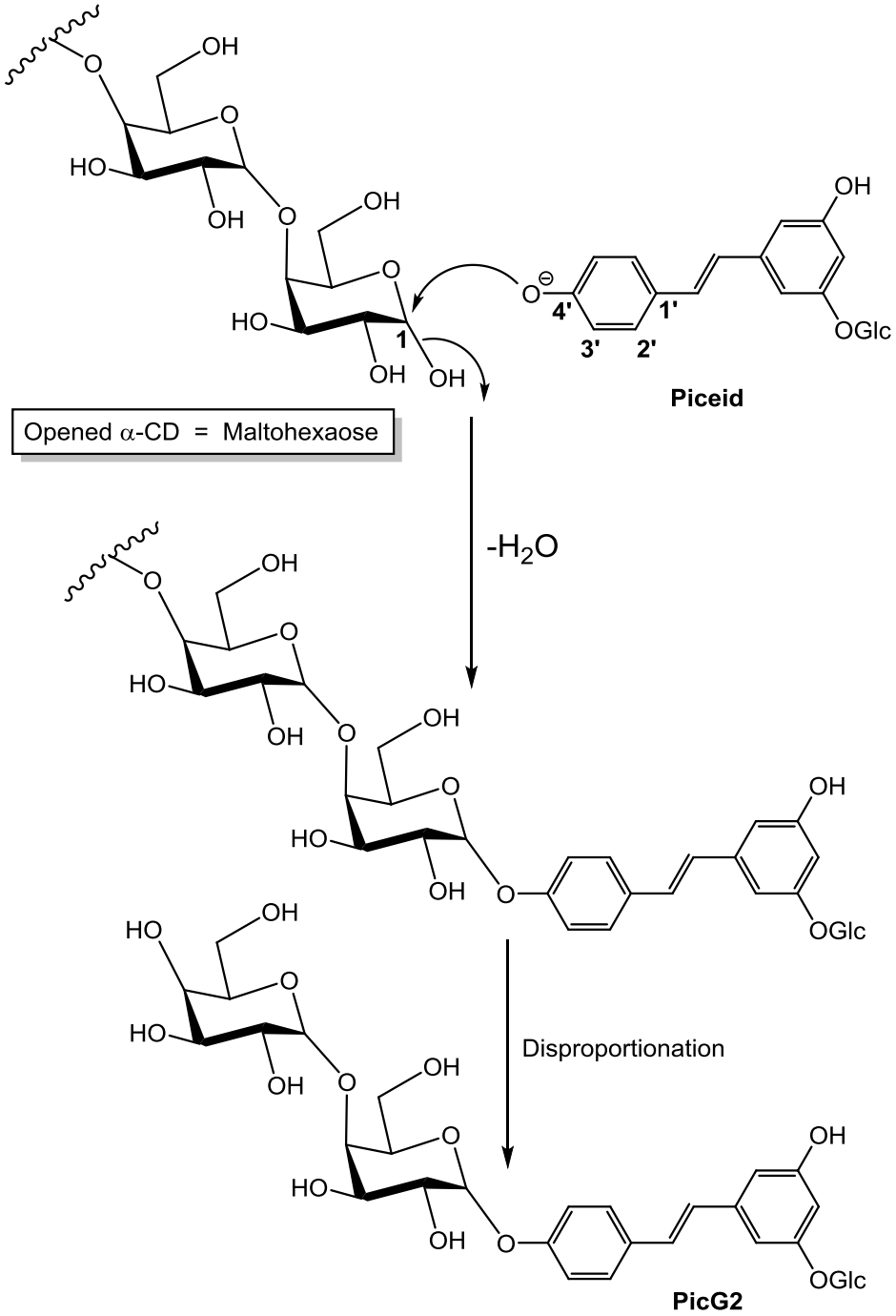
Piceid
Opened α-CD = Maltohexaose
-H2O
Disproportionation
PicG2

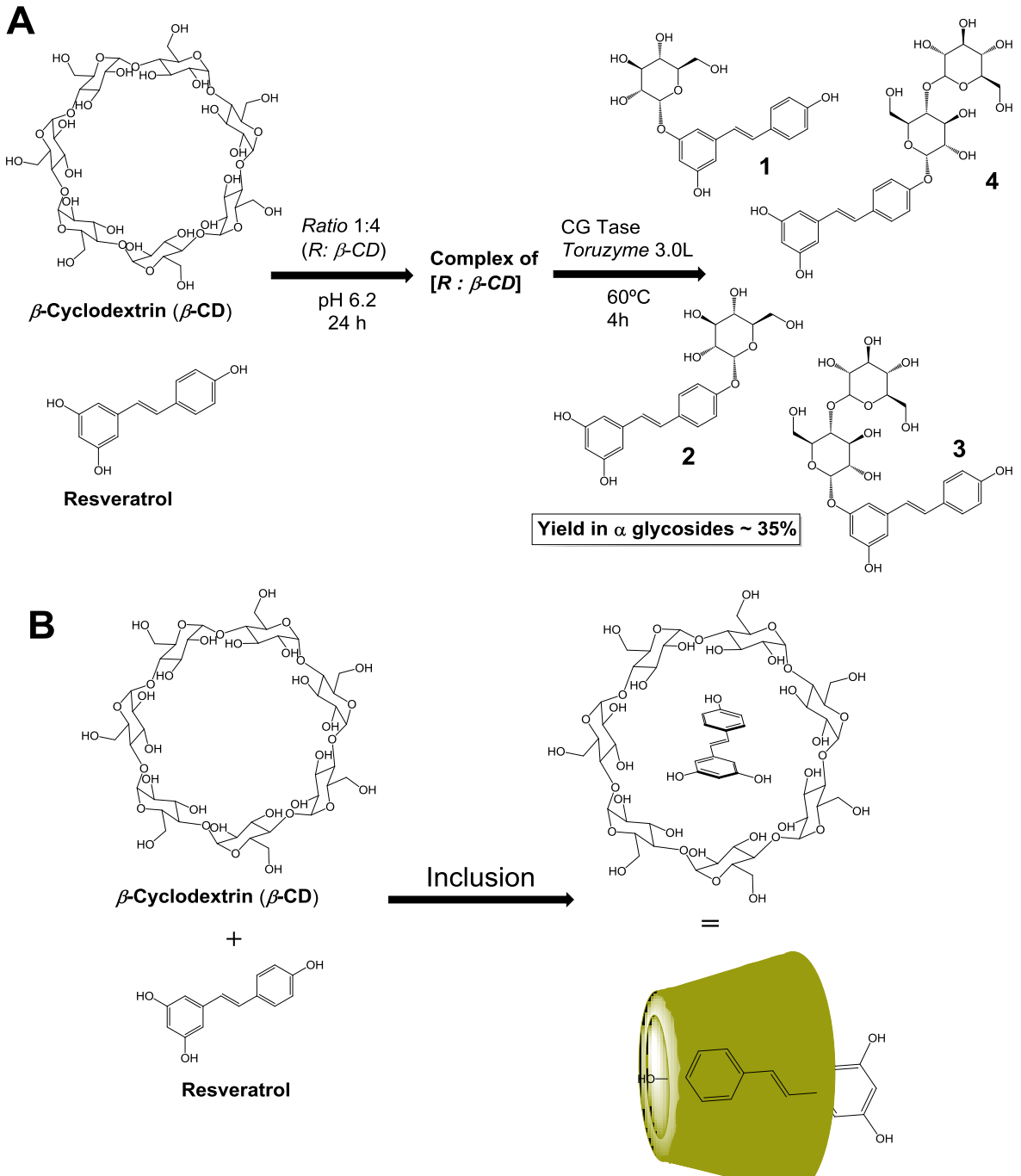
A
β-Cyclodextrin (β-CD)
Resveratrol
Ratio 1:4
(R: β-CD)
pH 6.2
24 h
Complex of
[R : β-CD]
CG Tase
Toruzyme 3.0L
60ºC
4h
1
2
3
4
Yield in α glycosides ~ 35%
B
β-Cyclodextrin (β-CD)
+
Resveratrol
Inclusion
=

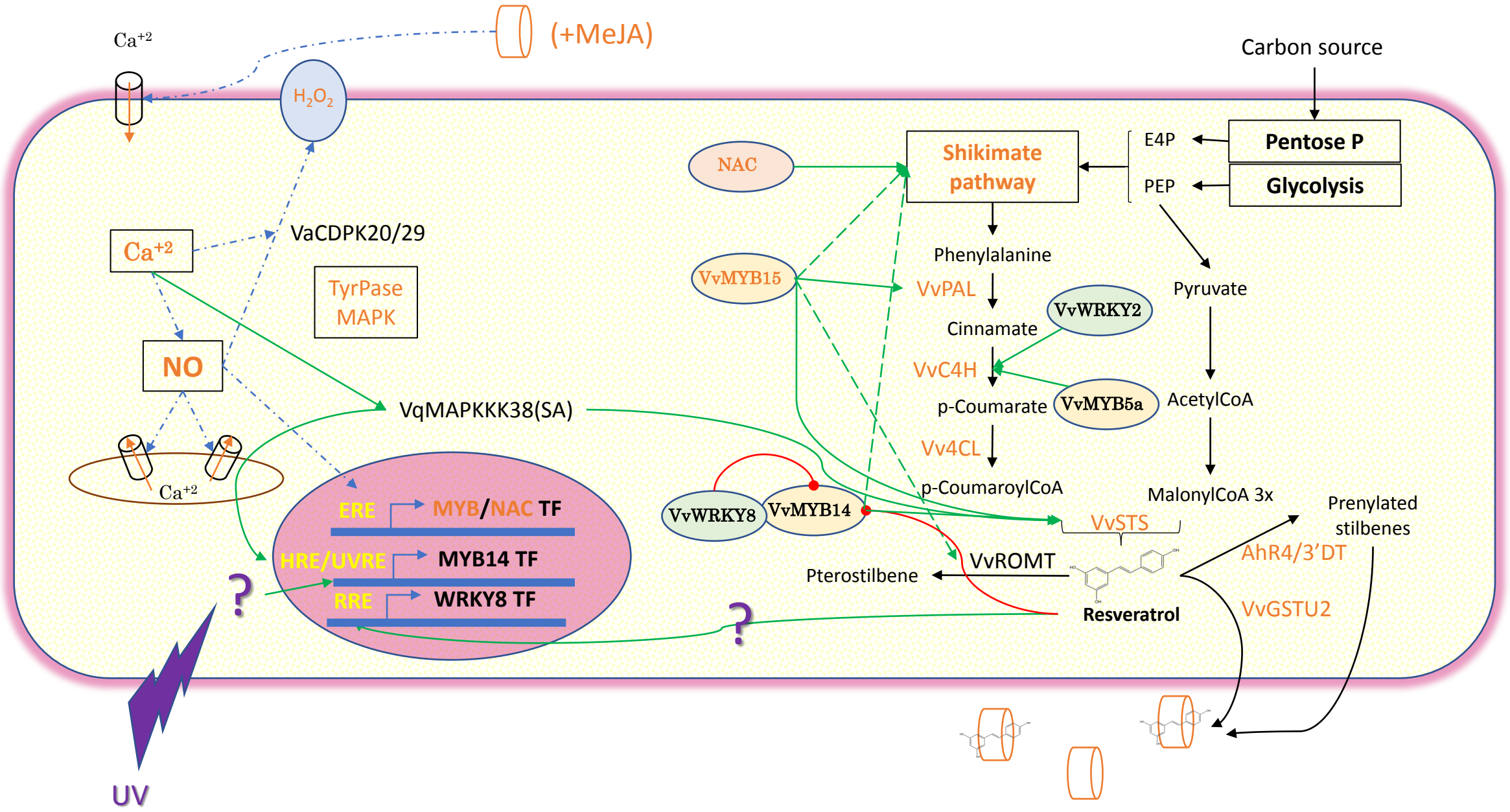
Ca+2
(+MeJA)
H2O2
Carbon source
Pentose P
Glycolysis
E4P
PEP
Shikimate pathway
NAC
VaCDPK20/29
Ca+2
TyrPase
MAPK
NO
VvMYB15
Phenylalanine
VvPAL
Cinnamate
VvWRKY2
Pyruvate
VvC4H
p-Coumarate
VvMYB5a
AcetylCoA
VqMAPKKK38(SA)
Ca+2
Vv4CL
p-CoumaroylCoA
MalonylCoA 3x
Prenylated stilbenes
ERE
MYB/NAC TF
VvWRKY8
VvMYB14
VvSTS
HRE/UVRE
MYB14 TF
VvROMT
AhR4/3'DT
Pterostilbene
RRE
WRKY8 TF
Resveratrol
VvGSTU2
?
?
UV

Table 1: Some parameters of stilbenes/cyclodextrins inclusion complexes

Abbreviations: K_s: stability constant; CD, cyclodextrin; β-CD, β-cyclodextrin; G2-β-CD, maltosyl- β-cyclodextrin; HP-β-CD, 2-hydroxypropyl-β-cyclodextrin; DM-β-CD, dimethylated-β-cyclodextrin; RAMEB-β-CD, randomized methylated- β-CD, Me-β-CD, methylated β-cyclodextrin; nr, not reported; PLGA, Poly (lactic-co-glycolic) acid; EE, entrapment efficiency; DL, drug loading; Resv-NS,resveratrol-nanosponge; Oxyresv-NS, oxyresveratrol-nanosponge; w/w,weight/weight ratio; GSH, glutathione

Type of CD	Stilbenes	Stoichio -metry	K_s values	Stilbene solubility increase	Stilbene loading	Stilbene release	Refs
β-CD	Resveratrol	1:1	2057 M^{-1}	2-fold	nr	nr	123
HP-β-CD	Resveratrol	1:1	1588 M^{-1}	nr	nr	nr	
DM-β-CD	Resveratrol	1:1	2604 M^{-1}	8-fold	nr	nr	
β-CD	Resveratrol	nr	4317 ± 338 M^{-1}	nr	nr	nr	93
G2-β-CD	Resveratrol	nr	5130 ± 421 M^{-1}	nr	nr	nr	
HP-β-CD	Resveratrol	1:1	3.17 x 10^5 M^{-1}	59500 fold	nr	nr	145
RAMEB-β-CD	Resveratrol	1:1	4.41 x 10^5 M^{-1}		nr	nr	
β-CD	Pinosylvin	1:1	5181 ± 233 M^{-1}	nr	nr	nr	129
HP-β-CD	Pinosylvin	1:1	12112 ± 761 M^{-1}	nr	nr	nr	
β-CD	Pterostilbene	1:1	8120 ± 440 M^{-1}	nr	nr	nr	119
HP-β-CD	Resveratrol	1:1	24880 ± 1020 M^{-}	nr	nr	nr	
HP-β-CD	Pterostilbene	1:1	17520 ± 981 M^{-1}	8 fold	nr	nr	
β-CD	Resveratrol	1:1	1815 M^{-1}	nr	nr	nr	131
HP-β-CD	Resveratrol	1:1	6778 M^{-1}	nr	nr	nr	
HP-β-CD	Resveratrol	1:1	3189 M^{-1}	increases with CD concentration	nr	nr	134
HP-β-CD	Resveratrol	nr	nr	nr	nr	nr	137
β-CD	Resveratrol	nr	nr	8.55 to 12.57 fold depending on CD concentration	nr	nr	143
HP-β-CD	Resveratrol	nr	nr	24.31 to 50.49 fold depending on CD concentration	nr	nr	

HP-β-CD HP-β-CD HP-β-CD	Resveratrol Pterostilbene Pinosylvin	1:1 1:1 1:2	1682 ± 49 M^{-1} 11730 ± 13 M^{-1} 14 ± 2.3 M^{-1}	4-6 log fold-increase	nr nr nr	nr nr nr	121
Sulfobutylether-β-CD	Resveratrol	1:1	10114 M^{-1}	37 fold (from 0.03 mg/mL to 1.1 mg/mL)	nr	nr	127
RAMEB-β-CD	Resveratrol	1:1	1482.9 ± 13.7 M^{-1}	400-fold	80%	Increased by 1.5-fold within 60 min	140
HP-β-CD	Piceatannol	1:1	14048 ± 702 M^{-1}	nr	nr	nr	120
HP-β-CD HP-β-CD	Resveratrol loaded in liposomes Resveratrol complexed with HP-β-CD and inclusion in liposomes Both complexation of resveratrol in liposomes and in HP-β-CD included in liposomes	nr nr nr	nr nr nr	nr nr nr	+3.08% +6.23% +11.6%	67.7% within 24h 100% within 24h 94.4% within 24h	94
β-CD Me-β-CD HP-β-CD	Oxyresveratrol Oxyresveratrol Oxyresveratrol	1:1 1:1 1:1	590.00 M^{-1} 606.65 M^{-1} 435.53 M^{-1}	nr nr nr	nr nr nr	nr nr nr	124
β-CD Me-β-CD HP-β-CD	Polydatin Polydatin Polydatin	1:1 1:1 1:1	798M^{-1} 1106 M^{-1} 1308 M^{-1}	6.4 fold-increase 7.9 fold increase 9 fold-increase	nr nr nr	nr nr nr	130
β-CD HP-β-CD	Oxyresveratrol Oxyresveratrol	1:1 1:1	1897.54 ± 81.14 M^{-1} 35864.72 ± 3415.89 M^{-1}	30 fold-increase (0.47 mg/mL to 14.44 mg/mL) 100 fold-increase (0.47 mg/mL to 47.33 mg/mL)	20% increase 20% increase	nr nr	125
HP-β-CD HP-β-CD HP-β-CD HP-β-CD	Resveratrol Oxyresveratrol Piceatannol Pterostilbene	nr	nr	nr	nr	nr	136

Sulfobutylether-β-CD + PLGA	Resveratrol	nr	nr	66 fold (from 0.03 mg/mL to 2.0 mg/mL)	EE: 29.1% DL: 0.72%	95.7% resv release within 30 min	144
γ-CD	Resveratrol	1:1	nr	9 fold-increase in lemon juice	nr	nr	135
NANOSPONGES							
Carbonyl nanosponge	Resveratrol	1:2/1:4	nr	33 fold-increase (Resv-NS 1:2) 48 fold-increase (Resv-NS 1:4)	30% increase (Resv-NS 1:2) 40% increase (Resv-NS 1:4)	5 fold-increase (Resv-NS 1:2) 9 fold-increase (Resv-NS 1:4) within 2h	100
Carbonyl nanosponge (NS-I) Carboxylate nanosponge (NS-II)	Resveratrol	nr	nr	51 to 161 and 167 μg/mL (NS-I 1:2;1:4) 51 to 152 and 156 μg/mL (NS-II 1:2;1:4)	91.52% (NS-I) 90.81 (NS-II)	3 fold-increases (NS-I and NS-II)	142
Carbonyl nanosponge in hydrogels	Curcumin and resveratrol	nr	nr	nr	nr	10 fold-increase including a lag phase with curcumin and 2.5 fold-increase with no lag phase with resveratrol compared to unloaded compounds	161
Carbonyl nanosponge	Resveratrol Oxyresveratrol	-	nr	3 fold for resveratrol (40 to 120 μg/mL) 2 fold for oxyresveratrol (600 to >1000 μg/mL)	9.47 to 14% increase (Resv-NS 1:2 and 1:6 w/w ratio) 11.93 to 16.78% increase (Oxyresv-NS 1:2 and 1:6 w/w ratio)	5 fold-increase (47.74% increase for resveratrol within 24h) *ca* 60% increase for oxyresveratrol within 24h	97
Carbonyl nanosponge	Resveratrol Oxyresveratrol	1:4	K_{app} (apparent association constant) values: Oxyresv-β-CD 1:4, 3917.89 ± 392.79 M^{-1} Resv-β-CD 1:4, 4466.48 ± 446.65 M^{-1}	nr	39.75% increase (Oxyresv-β-CD-NS 1:4)	Diffusion profile of Oxyresv-NS slower than that of free oxyresveratrol within 12h, pH dependent	141
α, β anr γ-CD polymers	Resveratrol	nr	nr	nr	4.5% increase for α and γ-CD polymers 6.7% increase for β-CD polymers	Respectively 11%, 6% and 12% resveratrol release for α, β and γ-CD polymers within 24h	88

GSH-responsive nanosponge	Resveratrol	nr	nr	4 fold-increase (46 to 201 μg/mL)	9.95% increase for Resv-β-CD-NS 1:2 (w/w) and 16.12% increase increase for Resv-β-CD-NS 1:4 (w/w)	2 fold-increase 5 fold-increase with 10 mM GSH 8 fold-increase with 20 mM GSH	99

Table 2: Some pharmacokinetic parameters of stilbenes or stilbene-cyclodextrin complexes

Abbreviations: C_{max}; maximum plasma concentration; T_{max}, maximal time to reach C_{max}; AUC, area under the curve; CMC, carboxymethyl cellulose; CD, cyclodextrin; β-CD, β-cyclodextrin; RAMEB-β-CD, randomized methylated- β-CD, Carbonyl-NS, carbonyl-nanosponge; Carboxylate-NS, carboxylate-nanosponge; HP-β-CD, 2-hydroxypropyl-β-cyclodextrin

Stilbene formulation	Doses (mg/kg)	Mode of administration	C_{max} (ng/mL)	T_{max} (min)	$AUC_{0\rightarrow t}$ (ng x h/mL)	Bioavailability, F (%)	Refs
CMC suspension	Resveratrol (25)	Oral	270 ± 60	5-15	485 ± 114	38.4 ± 9.02	
CMC suspension	Resveratrol (50)	Oral	430 ± 90	60-90	981 ± 49	38.8 ± 1.96	145
RAMEB-β-CD	Resveratrol (25)	Oral	860 ± 190	5-15	480 ± 24	38.0 ± 1.91	
RAMEB-β-CD	Resveratrol (50)	Oral	1750 ± 720	5-15	1009 ± 186	39.9 ± 7.38	
Resveratrol alone	Resveratrol (20)	Oral	496 ± 49	120	2080 ± 56	nr	
Carbonyl-NS	Resveratrol (20)	Oral	1107 ± 105	36	4145 ± 155	199.33 ($F_{relative}$)	142
Carboxylate-NS	Resveratrol (20)	Oral	1225 ± 111	30	3917 ± 263	188.37 ($F_{relative}$)	
HP-β-CD	Resveratrol (10)	Intravenous	15720 ± 3192	2	2836 ± 223	--	
HP-β-CD	Resveratrol (50)	Oral	1997 ± 1167	22	2352 ± 1737	16.68 ± 12.16	
HP-β-CD	Resveratrol (20)	Orotracheal	7156 ± 1637	7.8	5280 ± 565	92.95 ± 9.69	133
HP-β-CD	Resveratrol (2.3)	Inhalation	148 ± 86	142	390 ± 104	76.31 ± 10.74	

Table 3: Reported bioactivities of stilbenes/cyclodextrins inclusion complexes

Abbreviations: CD, cyclodextrin; NS, nanosponge; β-CD, β-cyclodextrin; HP-β-CD, 2-hydroxypropyl-β-cyclodextrin; DMBA, 7,12-dimethylbenz[a] anthracene; DM-β-CD, dimethylated-β-cyclodextrin; RAMEB-β-CD, randomized methylated-β-CD, Me-β-CD, methylated β-cyclodextrin; nr, not reported; PLGA, poly (lactic-co-glycolic) acid; Resv-NS, resveratrol-nanosponge; Oxyresv-NS, oxyresveratrol-nanosponge; DMSO, dimethylsulfoxide; w/w, weight/weight ratio; GSH-Resv-NS, glutathione responsive nanosponge

Stilbenes	Type of study	Type of CD or NS	Biological input	Refs
Resveratrol	*in vitro*	β-CD HP-β-CD	No significant increase in DPPH radical scavenging and antioxidant activities between resveratrol and Resv-β-CD or resveratrol and Resv-HP-β-CD Better efficiency of Resv-HP-β-CD against Resv- β-CD regarding antiradical and antioxidant activities	131
Resveratrol	*in vitro*	HP-β-CD	No significant increase in antiradical and lipoperoxidation activities between resveratrol and Resv-HP-β-CD Significant increase in resveratrol accumulation in porcine skins with use of Resv-HP-β-CD	134
Resveratrol	*in vitro* and *in vivo*	HP-β-CD in suspension in a cream (Resv-HP-β-CD-cream) or in a mouthwash (Resv- HP-β-CD-mouthwash)	Higher cytotoxicity of Resv-CD formulations compared to resveratrol on DMBA-induced oral squamous cell carcinoma (HCPC-I cell line) *in vitro* (24-72 h) *In vivo* prevention of exophytic lesions displaying oral squamous cell carcinoma characters. Order efficiency was: Resv-HP-β-CD-cream> Resv- HP-β-CD-mouthwash> free Resv	137
Resveratrol	*in vitro*	Carbonyl-β-CD-NS	Higher cytotoxicity of Resv-NS compared to resveratrol on DMBA-induced cancer cells of buccal mucosa (HCPC-I cell line) Higher permeation of Resv-NS through pig skin Two-fold higher accumulation of Resv-NS in rabbit mucosa	100
Resveratrol	*in vitro*	β-CD HP-β-CD	Dramatic morphological alterations of cell membranes of HeLa (human cervical carcinoma) cells with CD formulations of resveratrol but not with free resveratrol Decreased viability of HeLa cells and Hep3B (human hepatocellular liver cancer) cells with CD resveratrol formulations *vs* low cell viability inhibition with free resveratrol	143
Resveratrol	*in vitro*	Sulfobutylether-β-CD	Weak decrease (-65%) in the cell viability of human breast cancer cells (MCF-7 cell line) with the CD resveratrol inclusion complex when compared to resveratrol alone (-50%) within 72 h	127
Resveratrol	*in vitro*	RAMEB-β-CD	Strong antioxidant activity of resveratrol and Resv-CD but without any significant differences between free and internalized resveratrol No significant differences reported in the reduction in cell viability of Caco-2 cells (human epithelial colorectal carcinoma) cells between free and CD-included resveratrol	140
Resveratrol	*in vitro*	i) Resveratrol loaded in liposomes (RL) ii) Resveratrol complexed with HP-β-CD and inclusion in liposomes (RCL) iii) Both internalization of resveratrol in liposomes and in HP-β-CD and inclusion in liposomes (RL-CL)	Antiproliferative effect on HT-29-colon cancer cells within 24 h. All inclusion complexes (RL, RCL and RL-CL) displayed higher antiproliferative activities than free resveratrol. The increase in cytotoxicity was in the following order: RL-CL> RCL>RL>R	94

Pterostilbene	*in vivo*	HP-β-CD	Preservation of left ventricular function in infarcted rats following oral administration of the pterostilbene-HP-β-CD. No comparison with free pterostilbene was made precluding any conclusion regarding the effect of the inclusion process	152
Polydatin (3-*O*-β-D-resveratrol glucoside)	*in vitro*	β-CD Me-β-CD HP-β-CD	Increased antioxidant activity (as determined by measuring reducing power values) of inclusion complexes with polydatin than free polydatin in the following order: HP-β-CD>Me-β-CD>β-CD Increased DPPH radical scavenging activity of inclusion complexes with polydatin than free polydatin in the following order: HP-β-CD> Me-β-CD> β-CD	130
Resveratrol	*in vitro*	Carbonyl-β-CD nanosponge (Resv-NS-I) Carboxylate-β-CD nanosponge (Resv-NS-II)	Decrease of the cell viability (1.7-fold lower IC_{50} values) of human breast adenocarcinoma cells (MCF-7 cell line) with the CD resveratrol nanosponges, Resv-NS-I and Resv-NS-II, when compared to resveratrol alone	142
Resveratrol and oxy-resveratrol	*in vitro*	Carbonyl-β-CD nanosponge for resveratrol (Resv-NS) and oxyresveratrol (Oxyresv-NS)	Increased DPPH radical scavenging activity of inclusion nanosponges (Resv-NS and Oxyresv-NS) compared to free stilbenes Decrease of the cell viability of DU-145 prostate cancer cells upon stilbene inclusion with nanosponges compared to free stilbenes	97
Resveratrol and curcumin	*in vitro*	Carbonyl-β-CD nanosponge	Dose-dependent decrease in the cell viability of MCF-7 human breast adenocarcinoma cells with Resv-NS and curcumin-NS, respectively	161
Resveratrol	*in vivo*	Vectisol® (β-CD)	Beneficial effects upon kidney transplantation in a porcine model: slow-down of the loss of renal functions and beginning of histological lesions, decrease of apoptosis and oxidative stress Improvement of kidney preservation	132
Resveratrol	*in vivo*	Polymerized α, β and γ-CDs	Prolonged antioxidant effect of resveratrol on intracortical microelectrodes used for neurological diseases' treatment	88
Pterostilbene	*in vitro*	HP-β-CD	7.5 fold-decrease of the minimum inhibiting concentration and 4 fold-decrease of the minimum bactericidal concentration with pterostilbene CD-inclusion *vs* free pterostilbene in DMSO against *Fusobacterium nucleatum*, a periodontitis-associated pathogen	136
Oxy-resveratrol	*in vitro*	Carbonyl-nanosponge	1.5 fold-increase, 4 fold-increase and 6 fold-increase in the inhibition of cell viability of, respectively, prostate (PC-3) cancer cell line and colon (HT-29 and HCT-116) cancer cell lines with oxyresveratrol nanosponges *vs* free oxyresveratrol	141
Resveratrol	*in vitro*	Sulfobutylether-CDs + PLGA	15.39 fold- decrease in the IC_{50} against cell viability of non-small cell lung cancer (NSCLC) A549 cell line and 50 fold-decrease for the H358 cell line *vs* unloaded resveratrol. 1.7-fold increase in caspase-3 levels in the A549 cancer cell line *vs* unloaded resveratrol.	144

Resveratrol	*in vitro*	GSH-responsive nanosponge	Preferential entry of GSH-Resv-NS in cancer cells No toxicity of unloaded nanosponges on normal human fibroblasts Decreased viability of OVCAR3 human ovarian cancer cells and MDAMB231 human triple-negative breast cancer cells with GSH-Resv-NS compared to normal human fibroblasts and normal MCF10A human mammary epithelial cells	99
Resveratrol	*in vitro*	γ-CD	Conservation over time of the antiradical $ABTS^{\cdot+}$ capacity of lemon juice with γ-CD resveratrol complexation compared to juice supplemented with free resveratrol	135

Table 4: Green synthesis of stilbene glucosides using cyclodextrins

Abbreviations: CD, cyclodextrin; α-CD, α-cyclodextrin; β-CD, β-cyclodextrin; CGTase, Cyclodextrin glucosyltransferase; nr, not reported; Pic, piceid; DMSO, dimethylsulfoxide

Reaction conditions	Stilbene acceptor	Glucosides obtained	Biological input and effect on solubility	Refs
Starch → CD as glucose donor in DMSO/Na acetate buffer 10:34 (V/V) at pH 5.6 and 60°C with the CGTase from *Thermoanaerobacter*	Resveratrol (200 mg)	3-*O*-α-D-glucosyl-resveratrol (28.4 mg); 4'-*O*- α-D-glucosyl-resveratrol (20.5 mg); 3-*O*-α-D-maltosyl-resveratrol (12 mg); 4'-*O*-α-D-maltosyl-resveratrol (10.5 mg); 4'-*O*-α-D-maltotriosyl-resveratrol (6.1 mg) and 3,4'-*O*-α-D-diglucosyl-resveratrol (4.1 mg)	Glucoside solubilities: 2 g/L, that is, 5.4 fold-increase and 67 fold-increase in solubility compared to piceid (0.37 g/L) and resveratrol (0.03 g/L). Decrease in the antioxidant activity of glucosides compared to resveratrol	169
α-CD as glucose donor in 0.02 M citrate phosphate buffer with 5% methanol (V/V) at pH 6.0 and 40°C with the CGTase from *Bacillus macerans*	Piceid (2.56 mM)	Numerous glucosylated derivatives of piceid ($PicG_2$, $PicG_3$, etc…) not quantified (peak areas)	nr	168
α-CD as glucose donor in 50 mM citrate buffer at pH 5.6 and 37°C with a CGTase of unspecified origin	4'-*O*-β-D-glucosyl resveratrol (50 mg)	4'-*O*-β-D-maltosyl-resveratrol; (30% yield); 4'-*O*-β-D-maltotriosyl-resveratrol; (22% yield); 4'-*O*-β-D-maltotetraosyl-resveratrol (12% yield) and 4'-*O*-β-maltopentaosyl-resveratrol (6% yield)	Increase in the Inhibition of the phosphodiesterase activity (IC_{50}= 112 μM for 4'-*O*-β-D-maltosyl-resveratrol) compared to resveratrol (187 μM)	166
Starch → CD as glucose donor in water + DMSO 20% (V/V) at 60°C with the CGTase from *Thermoanaerobacter*	Pterostilbene (5 mg)	4'-*O*-α-D-glucosyl pterostilbene (0.12 mg) and an uncharacterized pterostilbene diglucoside (0.06 mg)	Increase in pterostilbene aqueous solubility from 0 to 0.1 g/L. 40% decrease in the antioxidant activity of 4'-*O*-α-D-glucoside of pterostilbene as well as a significantly lower toxicity on HT-29 colon cancer cells compared to the aglycone	163
β-CD as glucose donor in 2-[*N*-morpholino-] ethanesulfonic acid buffer at pH 6.2 and 80°C with the CGTase from *Thermoanaerobacter*	Resveratrol (2 g)	Resveratrol (89.22 mg); 3-*O*-α-D-glucosyl-resveratrol (366.6 mg); 4'-*O*- α-D-glucosyl-resveratrol (255.5 mg); 3-*O*-α-D-maltosyl-resveratrol (137.9 mg); 4'-*O*-α-D-maltosyl-resveratrol (85.16 mg)	Reduced antioxidant activities of the 3 and the 4'-*O*-α-D-glucosides of resveratrol (respectively 40 and 70% of that of resveratrol)	164
β-CD as glucose donor in phosphate buffer at pH 6.2 and 80°C with the CGTase from CGTase from *Thermoanaerobacter.* Reaction mixture coupled to a membrane process	Resveratrol	Shift of the glucosylation yield from 35% to 50%	nr	165